Cardiovascular Magnetic Resonance in the Oncology Patient

Jennifer H. Jordan, PhD, MS, Ryan M. Todd, BS, Sujethra Vasu, MBBS, W. Gregory Hundley, MD

ABSTRACT

Patients with or receiving potentially cardiotoxic treatment for cancer are susceptible to developing decrements in left ventricular mass, diastolic function, or systolic function. They may also experience valvular heart disease, pericardial disease, or intracardiac masses. Cardiovascular magnetic resonance may be used to assess cardiac anatomy, structure, and function and to characterize myocardial tissue. This combination of features facilitates the diagnosis and management of disease processes in patients with or those who have survived cancer. This report outlines and describes prior research involving cardiovascular magnetic resonance for assessing cardiovascular disease in patients with or previously having received treatment for cancer. (J Am Coll Cardiol Img 2018;11:1150–72) © 2018 The Authors. Published by Elsevier on behalf of the American College of Cardiology Foundation. This is an open access article under the CC BY-NC-ND license (http://creativecommons.org/licenses/by-nc-nd/4.0/).

T he emerging field of cardio-oncology involves assessment of cardiovascular disease specific to patients with or surviving cancer (1). Cancer survivors experience a 5-fold increase in the risk for developing heart failure, myocardial infarction, pericardial disease, or valvular abnormalities compared with their siblings without cancer (2). Each disease process may be noninvasively assessed with cardiovascular magnetic resonance (CMR) to establish a diagnosis or to guide therapy to address cardiovascular disease (Central Illustration) (3-5). In this report, we review the use of CMR for assessing the heart and surrounding structures in patients with or surviving cancer suspected of having cardiac abnormalities.

THE ROLE OF CMR IN PATIENTS WITH MALIGNANCIES

Several cardiac abnormalities may result from cancer or its treatment that promote a CMR evaluation (Figure 1). Preserving left ventricular (LV) function is often critical to enable delivery of one of several cancer therapeutic options designed to improve overall survival in patients with cancer. Thus, measurement of ventricular volumes, left ventricular ejection fraction (LVEF), and mass is a frequent consideration for patients receiving cancer treatment.

Even though transthoracic echocardiography (TTE) and radionuclide scintigraphy are often used to measure LVEF in patients receiving potentially cardiotoxic chemotherapy (Central Illustration), CMR is useful when one needs to characterize the LV myocardium to determine the etiology of a reduced LVEF. Myocardial inflammatory or infiltrative processes (e.g., myocarditis, amyloid, or iron deposition) serve as examples for which serial CMR LVEF and tissue characterization measures may be beneficial (6-9). In addition, CMR may differentiate the etiology of a newly identified abnormal myocardial mass, evaluate a pericardial disease process, or determine the cause of a valve leaflet abnormality during the same examination when LVEF is measured.

PERFORMANCE OF CMR

Descriptions of CMR imaging techniques, acquisition parameters, and analysis methods are provided in one of several publications authored by the Society of Cardiovascular Magnetic Resonance, the American College of Cardiology, and the American Heart Association (7,8,10). As of 2018, suggested revisions to imaging protocols, analysis methods, and reporting structures are currently under development with the Society for Cardiovascular Magnetic Resonance, with expected release in late 2018 or

early 2019. Table 1 categorizes existing magnetic resonance methods into those that provide anatomic, functional, and tissue characterization information that is useful for diagnosing the conditions described within this review. Throughout the paper, tables are provided that highlight key CMR imaging methods and features.

At present, several CMR imaging techniques incorporate the administration of gadolinium-based contrast agents (GBCAs). It should be noted that the administration of GBCAs can be associated with 3 untoward conditions: 1) allergic reactions to the agents themselves (dependent on GBCA type) with an incidence of 1:10,000 to 1:40,000 in the general population; 2) a serious but rare risk for nephrogenic systemic fibrosis in those with renal insufficiency; and 3) recent findings related to the unknown clinical significance of the potential accumulation of gadolinium in the brain stem after repetitive administration of these agents (11-13). These risks should be considered when evaluating any patient undergoing a CMR examination, but particularly in patients with cancer who, like other populations, may receive repetitive GBCAs to assess the extent of their malignancies. Gadolinium-enhanced contrast studies may provide clarity for questions related to tissue characterization.

LV DYSFUNCTION

To date, LVEF is the most widely used measure for identifying LV dysfunction resulting from the administration of cancer therapeutics (14,15). Early cardio-oncology studies identified that declines in LVEF after anthracycline administration are associated with development of congestive heart failure (16). Noninvasively, LVEF may be measured using radionuclide multiple-gated acquisition, 2-dimensional (2D) and 3-dimensional (3D) TTE, cardiac computed tomography, and CMR (5,17-21).

Reductions in LVEF after anthracycline treatment were first observed with radionuclide multiple-gated acquisition scans in the 1970s (16,22). Because radionuclide multiple-gated acquisition and cardiac computed tomography incorporate ionizing radiation, a limitation in patients who may be exposed to ionizing radiation exposure for treatment of their cancer, the use of TTE and CMR is increasingly preferred for performing serial measurements of LVEF during receipt of potentially cardiotoxic chemotherapy (23).

CMR measures of LVEF are most frequently quantified from a contiguous short-axis series of slices spanning the cardiac apex to its base using a steady-state free precession cine white-blood imaging technique (Table 2). The LV endocardial border contours from the end-diastolic and end-systolic frames in the cine sequence are used to provide LV cavity areas for each slice. By multiplying the area from the corresponding end-diastolic or end-systolic frame by the slice thickness, a volume for each slice of the cine sequence is obtained. By summing the volumes of all the slices and accounting for the interslice gaps, one can derive left ventricular end-diastolic volume (LVEDV) and left ventricular end-systolic volume (LVESV) using the modified Simpson rule (10). The LVEF is then calculated by subtracting LVESV from LVEDV and dividing this value (LV stroke volume) by LVEDV (10).

Serial CMR imaging studies of women treated for breast cancer after receipt of anthracycline-based chemotherapy have demonstrated declines in LVEF both during and 12 to 24 months after initiating therapy (Table 3). Importantly, some studies have indicated early declines in LVEF 1 month into therapy, which translates into receipt of only 1 or 2 doses of an anthracycline agent. The prognostic implications of these acute changes are not yet known.
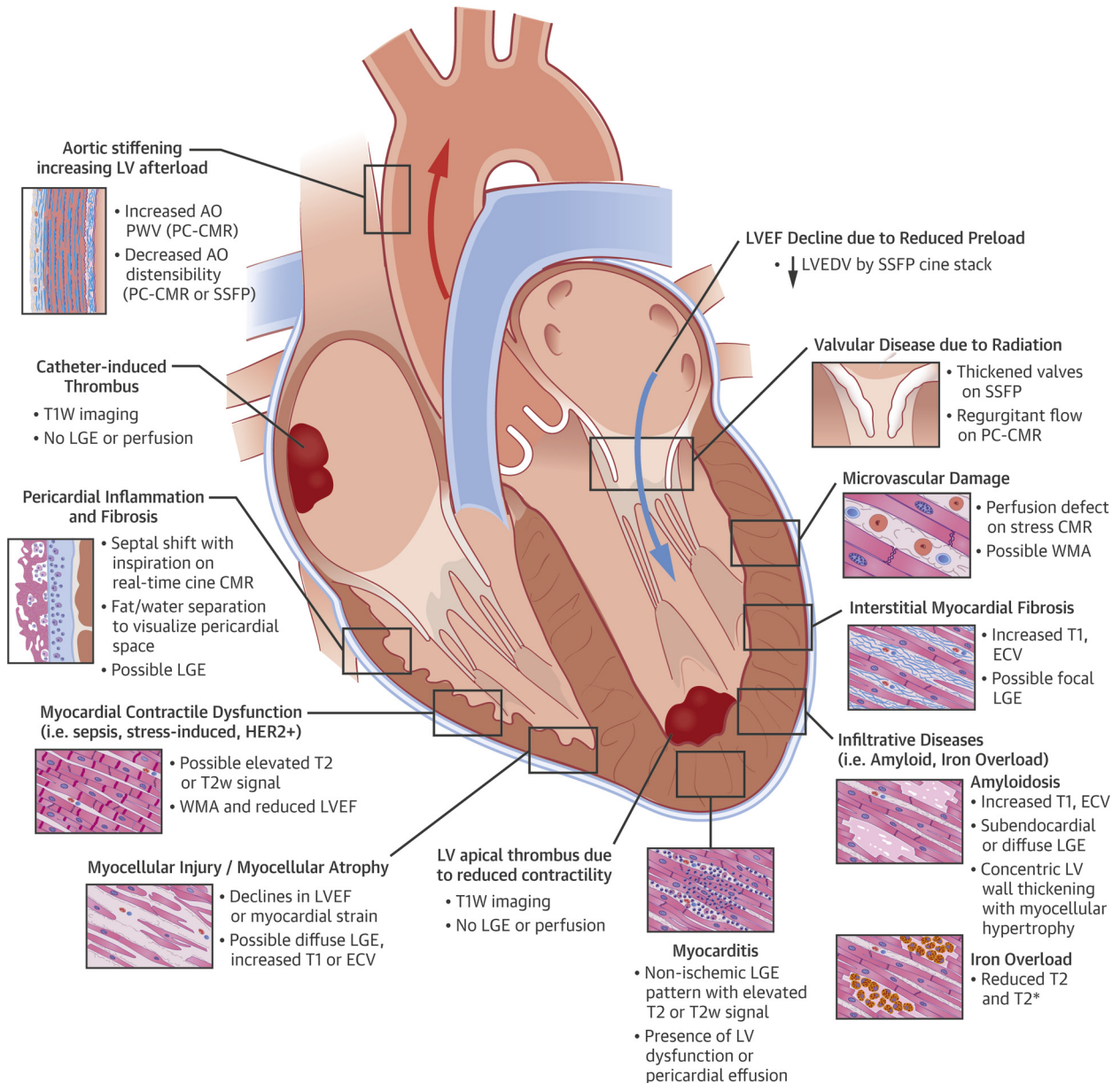
Several primarily echocardiography based algorithms have been proposed for monitoring cardiotoxicity (defined as LVEF decline >10% to <53%) in the setting of trastuzumab and other targeted therapies (14,24,25). Recent consensus statements recommend baseline evaluation of LVEF with 2D or 3D echocardiography. If the LVEF is <53% by echocardiography or if poor image quality prohibits measurement of LVEF, CMR is recommended (14). Similar algorithms are proposed for surveillance of patients with cancer and survivors (14).

CMR is of particular advantage in this population because of its high spatial and temporal resolution, reproducibility, and accuracy for LVEF quantification to detect subclinical declines in LVEF, which may occur as early as 1 month after the receipt of cardiotoxic therapies (26,27). In the St. Jude Lifetime Cohort of adult survivors of pediatric cancers, Armstrong et al. (28) performed a head-to-head comparison of 2D and 3D echocardiographic measures with CMR measures of LVEF. The results of this study indicated that LVEF values derived from 2D echocardiography overestimated the mean LVEF by

CENTRAL ILLUSTRATION   Adverse Cardiovascular Effects Related to Cancer Treatment and Key Cardiovascular Magnetic Resonance Features

Jordan, J.H. et al. J Am Coll Cardiol Img. 2018;11(8):1150–72.

This figure illustrates cardiovascular complications that may be found in patients with cancer or survivors related to their cancer treatment. Cardiovascular magnetic resonance (CMR) imaging may be useful to not only identify these disease processes but also comprehensively assess their impact on cardiovascular function. AO = aorta; ECV = extracellular volume; HER2 = human epidermal growth factor receptor 2; LA = left atrium; LGE = late gadolinium enhancement; LV = left ventricle; LVEDV = left ventricular end-diastolic volume; LVEF = left ventricular ejection fraction; PA = pulmonary artery; PC = phase-contrast; PWV = pulse-wave velocity; RA = right atrium; RV = right ventricle; SSFP = steady-state free precession; T1W = T1-weighted; T2w = T2-weighted; WMA = wall motion abnormality.

FIGURE 1 The Role of Cardiovascular Magnetic Resonance in Patients With Cancer

The Role of Cardiac MRI in Patients with Cancer

- LV Contractile Dysfunction (↓LVEF or strain)
- LV Myocardial Volume or Mass
- Evaluation of a Cardiac Mass
- Valvular Disease
- Right Ventricular Function
- Pericardial Disease

EDV ↓
ESV ↑

- Volume depletion
- Diastolic dysfunction

Perfusion Deficit
- Microcirculatory dysfunction
  - Atherosclerosis
  - Endothelial dysfunction
- Epicardial coronary disease
  - Atherosclerosis
  - Endothelial dysfunction
  - Vasospasm

Myocardial Fibrosis
- Replacement fibrosis
  - Infarction
- Interstitial fibrosis
  - Chronic medical condition, e.g. HTN
  - Cancer therapy associated

Infiltrative Disorder
- Amyloid
- Iron deposition

Myocellular Dysfunction

Increased Afterload
- Aortic stiffening
- Vascular resistance

Myocellular Injury
- Mitochondrial dysfunction
- Oxidative stress
- Apoptosis

Sepsis

Receptor-mediated Dysfunction
- Type II injury (Trastuzumab)

Stress-induced Cardiomyopathy
- Acute onset
- Treatment-related onset

Myocarditis
- Autoimmune
- Infectious

Cardiovascular magnetic resonance imaging may be used to identify a number of cancer-associated conditions or treatment-related effects. EDV = end-diastolic volume; ESV = end-systolic volume; HTN = hypertension; LV = left ventricular; LVEF = left ventricular ejection fraction; MRI = magnetic resonance imaging.

TABLE 1 Categories for Cardiovascular Magnetic Resonance Imaging in Cardio-Oncology

Anatomy	Function	Tissue Characterization

• Dark-blood T1-weighted imaging
• Dark-blood T2-weighted imaging
• Single- and multiphase white-blood SSFP imaging in long-axis chamber views, short-axis (for left ventricle), and axial (for right ventricle) orientations to define endocardial border
• Fat/water separation imaging to identify pericardium and distinguish from surrounding fat
	• Cine white-blood SSFP imaging in short-axis view (left ventricle) or axial orientation (right ventricle) for assessment of wall motion abnormalities and calculation of end-diastolic volume, end-systolic volume, stroke volume, ejection fraction, and mass
	• Real-time cine white-blood imaging to evaluate function and identify ventricular independence and septal shift in the setting of pericardial constriction
	• Phase-contrast assessment of valvular regurgitation or stenosis
	• Short- and long-axis strain imaging (tagged or feature-tracking methods)
		Noncontrasted
		• Fat/water separation imaging to identify pericardium and distinguish from surrounding fat
		• Native T1 mapping*
		• T2 mapping*
		• T2* mapping*
		Contrasted
		• Contrast-enhanced T1 mapping for ECV calculation*
		• Late gadolinium enhancement imaging to assess
		  ○ Patterns of enhancement in myocardium
		  ○ Extent of fibrosis or inflammation
		  ○ Pericardial tumor invasion
		  ○ Valve mass (with and without prolonged inversion time)

Imaging sequences are categorized into use for anatomic, functional, and tissue characterization applications. *Specialized imaging sequences used less in daily clinical practice that may be available only for research purposes at some centers.

ECV = extracellular volume; SSFP = steady-state free precession.

TABLE 2 Cardiovascular Magnetic Resonance Imaging Methods to Assess the Left Ventricle in Cardio-Oncology

Left Ventricle
Anatomy
• Single-phase white-blood imaging in 2-, 3-, and 4-chamber views
• Cine white-blood imaging in short-axis orientation for assessment of LVEDV, LVESV, stroke volume, LVEF, and LV mass
Function/flow
• Cine white-blood imaging in short-axis orientation for assessment of LV wall motion abnormalities
• Short- and long-axis strain imaging (tagged or feature-tracking methods)
Tissue characterization
• Native T1, T2, and T2* mapping
• Late gadolinium enhancement imaging
• Post-gadolinium contrast-enhanced T1 mapping

LV = left ventricular; LVEDV = left ventricular end-diastolic volume; LVEF = left ventricular ejection fraction; LVESV = left ventricular end-systolic volume.

5%. Importantly, 11% of patients were misclassified as exhibiting LVEFs <50% when the value exceeded 50% by 3D methods.

In the same study, LV volumes and LVEF generated from 3D echocardiography exhibited less variance than 2D echocardiography, but the investigators concluded that neither method reached the desired level of accuracy necessary to reliably identify 5% changes in LVEF that may be necessary to screen patients for LV dysfunction upon receipt of

cardiotoxic chemotherapies (28). Because of an absence of acoustic window limitations and accurate determination of 3D volumes, LVEF measures obtained with CMR provide a nice alternative for identifying small changes in LVEF that may occur as a results of the receipt of potentially cardiotoxic chemotherapy used to treat cancer. In addition, CMR measures of LVEF are particularly useful when echocardiographic windows are difficult or echocardiographic LVEF quantification is borderline.

Recently, several consensus documents have proposed algorithms for using TTE to follow patients scheduled to receive anthracycline-based regimens. These clinical management algorithms suggest obtaining LVEF measurements at baseline, upon completion of therapy, and again 6 months after completing therapy. For those receiving trastuzumab, it is recommended to obtain baseline evaluations of LVEF with repeated assessments every 3 months during therapy (14). At present, CMR-derived algorithms have not been incorporated into these recommendations unless transthoracic echocardiographic images are of poor quality or a low LVEF assessment is obtained with TTE. It should be noted that CMR normative values for LVEF are higher than those obtained with TTE (20),

TABLE 3 Left Ventricular Ejection Fraction Decreases and Reported Cardiotoxicity Are Variable in Serial Imaging Studies of Women With Breast Cancer Treated With Anthracyclines by Different Imaging Modalities
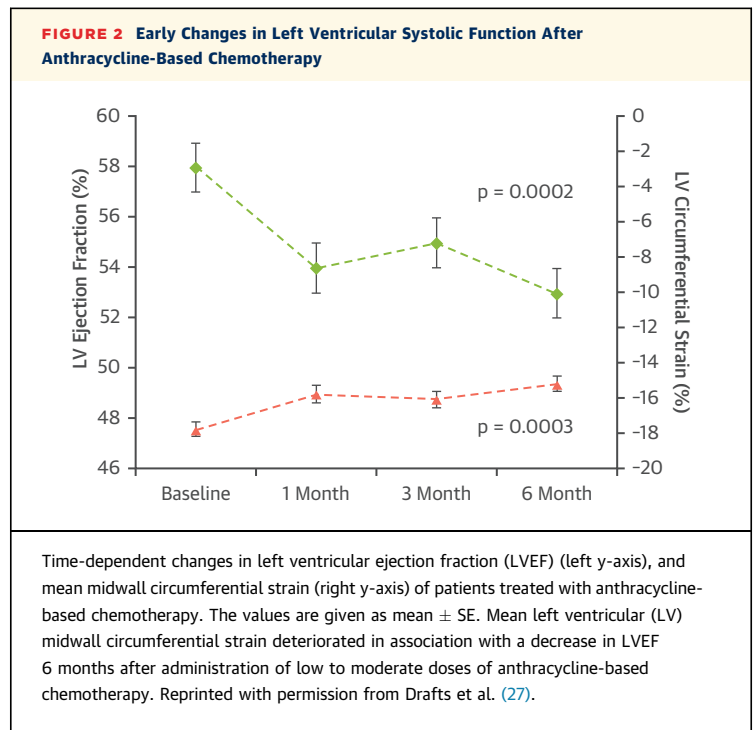
Imaging Modality First Author (Ref. #)	n, Total	% Breast Cancer	Age, yrs	Treatment	Follow-Up, months	Baseline LVEF, %	Follow-Up LVEF, %	LVEF Decline, %	CT
MUGA									
Cottin et al. (141)	60	47	50 (23–72)	Anthracycline	1	57 ± 5	55 ± 6	2	NR
Lapinska et al. (142)	71	100	53 (38–71)	Anthracycline + cyclophosphamide (n = 47)	6	62.7 ± 4.4	59.5 ± 6.1	3	NR
				Anthracycline + docetaxel (n = 24)		63.7 ± 5.2	61.7 ± 5.3	2	
Feola et al. (143)	53	100	55 (28–73)	Anthracycline	24	63.9 ± 4.8	53.1 ± 6.6	11	n = 13 (25%)
Echocardiography									
Fallah-Rad et al. (62)	42	100	47 ± 9	Anthracycline + trastuzumab	6	62 ± 5 (normal LVEF, n = 32)	64 ± 4 (normal LVEF, n = 32)	No decline	n = 10 (24%)
						64 ± 3 (CT, n = 10)	42 ± 4 (CT, n = 10)	22	
Stoodley et al. (144)	52	100	49 ± 9	Anthracycline	4–6	58.6 ± 2.6	56.0 ± 2.8	No decline	n = 0 (0%)
CMR									
Fallah-Rad et al. (62)	42	100	47 ± 9	Anthracycline + trastuzumab	12	65 ± 3 (normal LVEF, n = 32)	63 ± 5 (normal LVEF, n = 32)	No decline	n = 10 (24%)
						66 ± 5 (CT, n = 10)	47 ± 4 (CT, n = 10)	22	
Drafts et al. (27)*	53	42	50 ± 2	Anthracycline	6	58 ± 1	53 ± 1	5	n = 14 (26%)
Chaosuwannakit et al. (43)	40	48	52 ± 11	Anthracycline	4	58.6 ± 6.3	53.9 ± 6.4	5	NR
Wassmuth et al. (26)*	22	36	43 (17–66)	Anthracycline	1	67.8 ± 1.4	58.9 ± 1.9	9	n = 6 (27%)

Values are median (range) or mean ± SD unless otherwise noted. *Mean ± SE.

CMR = cardiovascular magnetic resonance; CT = cardiotoxicity; LVEF = left ventricular ejection fraction; MUGA = multiple gated acquisition ventriculography; NR = not reported.

and thus uncertainty remains as to the particular CMR-derived LVEF measurement that indicates the presence of myocardial injury due to a specific cancer treatment.

There are several concerns related to simply using a measure of LVEF to define the presence or absence of "cardiotoxicity" upon receipt of chemotherapy or radiation therapy. First, many cancer therapies, including radiation therapy, may induce processes (e.g., valvular or pericardial disease, myocellular injury, LV diastolic dysfunction, epicardial coronary artery or microcirculatory injury) that do not precipitate an early change in LVEF (29,30). For example, upon receipt of potentially cardiotoxic chemotherapy, LV regional diastolic relaxation may decline prior to change in LVEF. It is important to note, however, that data regarding LV diastolic dysfunction secondary to cancer treatment are limited, and CMR assessment of diastolic dysfunction is used primarily in the research environment. Clinically, TTE is the more frequently used method to identify LV diastolic function.

Second, patients with high grades of myocellular injury on biopsy may not necessarily display marked changes in LVEF (31). LV longitudinal myocardial strain obtained with TTE may deteriorate prior to or occur along with asymptomatic LVEF depression (18,32). Recent evidence suggests that LV global longitudinal strain (GLS) measured with feature-tracking CMR may also identify early LV dysfunction. Romano et al. (33) demonstrated that CMR-derived GLS was a strong, independent predictor of all-cause mortality in those with ischemic and nonischemic dilated cardiomyopathy after accounting for both LVEF and late gadolinium enhancement (LGE) burden. Recent work by Jolly et al. (34) used short-axis cine imaging to measure 3-month serial changes in global LV circumferential strain with feature tracking in 72 patients undergoing chemotherapy using automated segmentation (34). Global LV circumferential strain worsened in patients at 3 months (−17.6 ± 3.1% vs. −18.8 ± 2.9%, p = 0.001) and was strongly correlated with changes in early subclinical declines in LVEF (r = 0.49, p < 0.0001) (34).
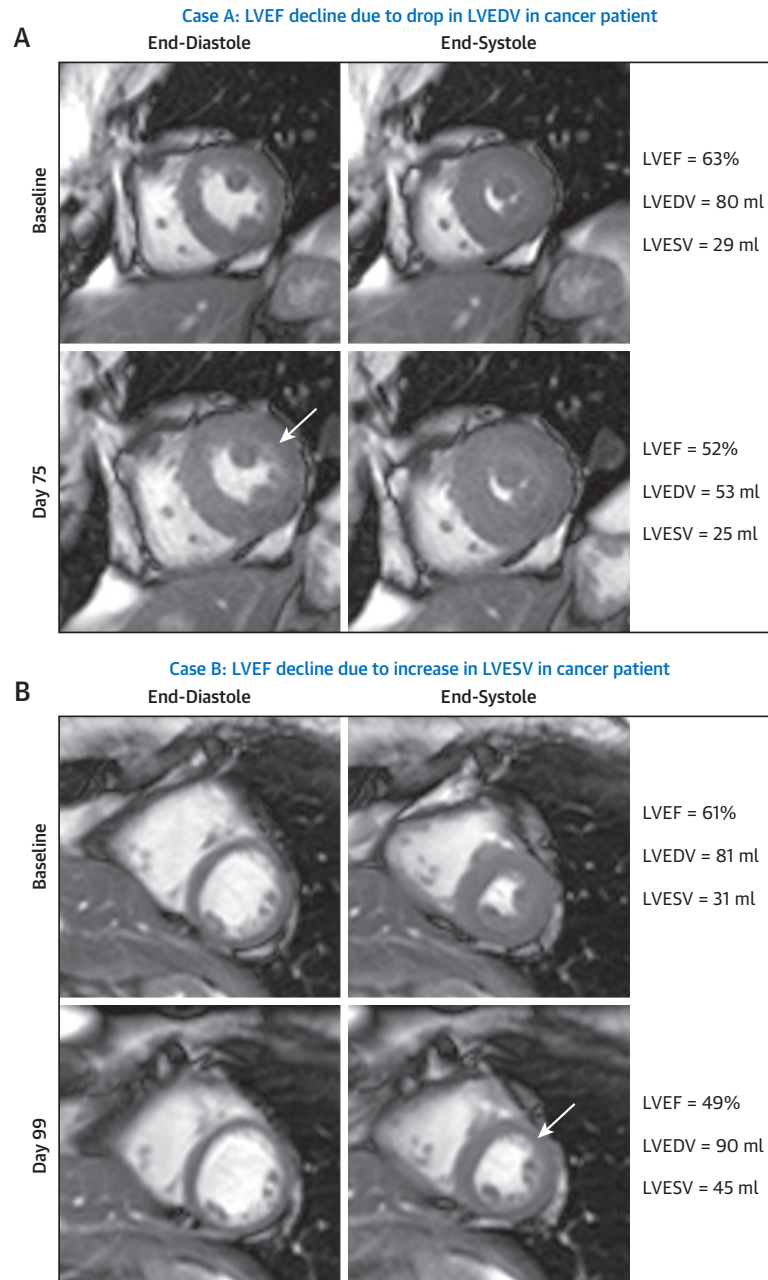
Serial CMR measures of LV myocardial strain may also be accomplished by either spatial modulation of magnetization or displacement encoding with stimulated echoes techniques (35,36). In a prospective study of 53 patients treated for breast cancer or hematologic malignancies, global LV circumferential strain measured by CMR deteriorated along with subclinical declines in LVEF within 1 to 6 months

FIGURE 2 Early Changes in Left Ventricular Systolic Function After Anthracycline-Based Chemotherapy

Time-dependent changes in left ventricular ejection fraction (LVEF) (left y-axis), and mean midwall circumferential strain (right y-axis) of patients treated with anthracycline-based chemotherapy. The values are given as mean ± SE. Mean left ventricular (LV) midwall circumferential strain deteriorated in association with a decrease in LVEF 6 months after administration of low to moderate doses of anthracycline-based chemotherapy. Reprinted with permission from Drafts et al. (27).

following the initiation of treatment with low to moderate doses of an anthracycline chemotherapeutic agent (**Figure 2**) (27). It is important to recognize that at present, CMR strain measures are not widely performed clinically. Future studies are needed to determine the prognostic value of abnormal GLS or circumferential myocardial strain by CMR in cardio-oncology patients.

Third, when assessing LVEF, one must consider whether a decline in LVEF occurs as a reduction in LVEDV or an increase in LVESV (**Figure 1**). Meléndez et al. (37) studied 120 patients with adult cancer 3 months after the administration of chemotherapy and observed that in those with LVEF declines >10%, nearly one-fifth experienced LVEF declines from isolated declines in LVEDV (**Figure 3**, Online Videos 1, 2, 3, and 4). In a subsequent analysis on a subset of these same subjects, Jordan et al. (38) observed that 16% of patients may experience deterioration in myocardial circumferential strain due to isolated declines in LVEDV (38). These data reflect the fact that LV myocardial strain measures (longitudinal, radial, or circumferential) are affected by LV pre-load and afterload. Patients receiving treatment for cancer can experience decreases in appetite, nausea, vomiting, or diarrhea, which reduces LV pre-load (manifest by a decrease in LVEDV), which can promote decrements in LVEF

1156   Jordan et al.
CMR in the Oncology Patient

JACC: CARDIOVASCULAR IMAGING, VOL. 11, NO. 8, 2018
AUGUST 2018:1150–72

FIGURE 3 Cardiovascular Magnetic Resonance Case Examples of Left Ventricular Ejection Fraction Due to Either a Decline in Left Ventricular End-Diastolic Volume or an Increase in Left Ventricular End-Systolic Volume After Chemotherapy

Cardiovascular magnetic resonance images demonstrating mid-short-axis white-blood slice acquired prior to treatment **(top)** and 3 months post-treatment **(bottom)**, with end-diastolic frames shown on the **left** and end-systolic frames shown on the **right**. **(A)** A case of a precipitous decline in left ventricular ejection fraction (LVEF) after 3 months of treatment due to a decline in left ventricular end-diastolic volume (LVEDV) of unknown origin in a 57-year-old white woman with a history of diabetes and hypertension who was treated with 2 cycles of sunitinib for metastatic renal cell carcinoma. As shown in this case example, the baseline LVEF was 63% (Online Video 1) and declined to 52% (Online Video 2) 75 days thereafter because of a change in LVEDV. **(B)** A case of anthracycline-mediated LV systolic dysfunction with a precipitous decline in LVEF 3 months after initiation of treatment. In this situation, LV end-systolic volume (LVESV) increased in a 59-year-old white woman with a history of smoking who was treated with anthracycline-containing chemotherapy for breast cancer. As shown in this case example, the baseline LVEF was 61% (Online Video 3) and declined to 49% (Online Video 4) 99 days thereafter because of a change in LVESV.

and myocardial strain (3,4,39). These data underscore the importance of reviewing LVESV and LVEDV when assessing LVEF and myocardial strain as indexes of LV dysfunction.

INCREASED LV AFTERLOAD LEADING TO DECREASES IN LVEF. Once LVEF decline due to an increase in LVESV is identified, one must consider whether the increase in LVESV is related to an abnormality intrinsic or extrinsic to the LV myocardium. Increased LV afterload represents a condition that may promote an increase in LVESV related to a factor extrinsic to the LV myocardium. Examples of conditions that increase LV afterload include scenarios that promote aortic stiffening or increased vascular resistance resulting from the administration of anthracycline agents, tyrosine kinase inhibitors, or endothelium receptor antagonists (3,40).

Aortic phase contrast imaging with CMR provides a noninvasive assessment of aortic flow and stiffness (41). Measurements obtained from phase contrast include pulse-wave velocity and aortic distensibility (41). With normal aging, these measures deteriorate as the aorta becomes less compliant and blood ejected from the left ventricle travels quicker through the vessel (41,42). Several studies of patients with breast cancer and hematologic malignancies undergoing chemotherapy treatment with anthracyclines, cyclophosphamide, and/or trastuzumab have shown elevated measures of pulse-wave velocity in the aorta and decreased ascending thoracic aortic distensibility (27,43,44). In another study of 29 patients with breast cancer receiving sequential anthracycline and trastuzumab treatment, aortic pulse-wave velocity increased 4 months after therapy but resolved 1 year thereafter (44). Anthracycline administration was associated with reduced ascending thoracic aortic distensibility (44). Although small in size, these prospective longitudinal studies demonstrate the potential utility of CMR to comprehensively evaluate vascular factors that may contribute to LV dysfunction.

INCREASES IN LVESV IN PATIENTS TREATED FOR CANCER. Myocellular dysfunction. There are several etiologies of myocellular dysfunction that may contribute to LV dysfunction in patients receiving potentially cardiotoxicity chemotherapy: myocarditis, stress-induced cardiomyopathy, modulation of myocardial contractility, sepsis, and myocellular injury.

Myocarditis. Myocarditis, an inflammatory disorder involving cardiomyocytes, can manifest as an abnormality of a particular cardiac serum biomarker, fatigue, chest pain, heart failure, arrhythmias, or sudden death (45). Myocarditis may result from viral infection, bacterial infection, or an autoimmune disorder (46). For example, data suggest that fulminant myocarditis may result from exposure to checkpoint inhibitors, particularly when they are used in combination (e.g., the combination of ipilimumab and nivolumab yielding a 0.27% incidence of fulminant myocarditis per Bristol-Myers Squibb database) (45,47,48).

CMR is a useful modality for identifying myocardial inflammation related to myocarditis. In general, 4 types of tissue characterization imaging strategies are used to identify myocarditis: contrast enhanced T1-weighted imaging and noncontrast T2-weighted, T1 mapping, and T2 mapping sequences. A combination of CMR methods incorporating T1, T2, and LGE criteria has sensitivity of 76% and specificity of 96% for identifying myocarditis with pathological confirmation (49,50). Tissue inflammation involves regional vasodilation, which results in an increased uptake of contrast agents during early phases. Therefore, the finding of increased early gadolinium enhancement using T1-weighted images is consistent with myocarditis (**Table 4**). An alternative approach is to incorporate a T1-weighted segmented inversion-recovery gradient-echo sequence to improve the signal intensity contrast between diseased and healthy myocardial regions. This imaging strategy may further improve the contrast between healthy and inflamed myocardium.

Because inflammatory cell injury leads to increased permeability of cellular membranes, T2-weighted global and regional edema imaging may be used to identify acute myocardial inflammation (6). In cases of myocarditis, LGE imaging reveals either high signal intensity, a rimlike pattern in the septal wall, or a subepicardial, patchy distribution in the free LV lateral wall. In addition, the presence of LV dysfunction or pericardial effusion (using steady-state free precession imaging with T2 sensitivity) is supportive of suspected myocarditis (6,51). In summary, differences in both signal intensity and distribution of enhancement with CMR tissue characterization techniques can identify myocarditis in patients with or surviving cancer.

Moslehi (47) demonstrated the appearance of autoimmune myocarditis has features similar to that observed from myocarditis related to an infectious etiology. A recent report by Mahmood et al. (52) describes an 8-center registry of myocarditis

TABLE 4	Key Cardiovascular Magnetic Resonance Features of Myocarditis
Rimlike pattern of LGE in septal wall or patchy, subepicardial LGE in LV lateral wall
Presence of LV dysfunction or pericardial effusion
Global or regional T2-weighted enhancement of left ventricle
LGE = late gadolinium enhancement; LV = left ventricular.

associated with immune checkpoint inhibitors. This new study indicates the prevalence of myocarditis was 1.14% with a median time of 34 days after initiating immunotherapy, more than twice that of an earlier study of myocarditis following immunotherapy (48). Although baseline screening electrocardiographic or echocardiographic assessments did not provide useful risk assessment for developing myocarditis, electrocardiographic changes and elevated troponin were common after myocarditis diagnosis (52). LGE patterns typical of myocarditis (subepicardial, midwall, diffuse) were observed in 27 patients (77%) with no significant difference in pattern frequency between those with and without subsequent cardiac events (52). Although CMR LGE may aid in diagnosis of myocarditis, current data suggest that LGE patterns do not predict outcomes in this population.

Stress-induced cardiomyopathy. A cause of LV dysfunction in patients with malignancies includes the occurrence of stress-induced transient LV dysfunction syndrome (TLVDS), or takotsubo cardiomyopathy. In TLVDS, patients with cancer may experience a somewhat acute but often rapidly reversible form of LV systolic function in the absence or presence of other forms of cardiovascular disease (53,54). This transient form of cardiomyopathy can mimic ST-segment elevation myocardial infarction in that patients can experience anginal-type chest pain, ST-segment changes, and LV regional wall motion abnormalities that more frequently but not exclusively involve the LV apex.

In 1 series of 50 patients with TLVDS compared with 50 age- and sex-matched patients who had experienced acute myocardial infarction, 18% of the patients with TLVDS had prior diagnoses of malignancy compared with fewer than 6% of those experiencing myocardial infarction (55). Importantly, as in other patients with TLVDS without cancer, it is primarily women with cancer who experience this condition as opposed to men.
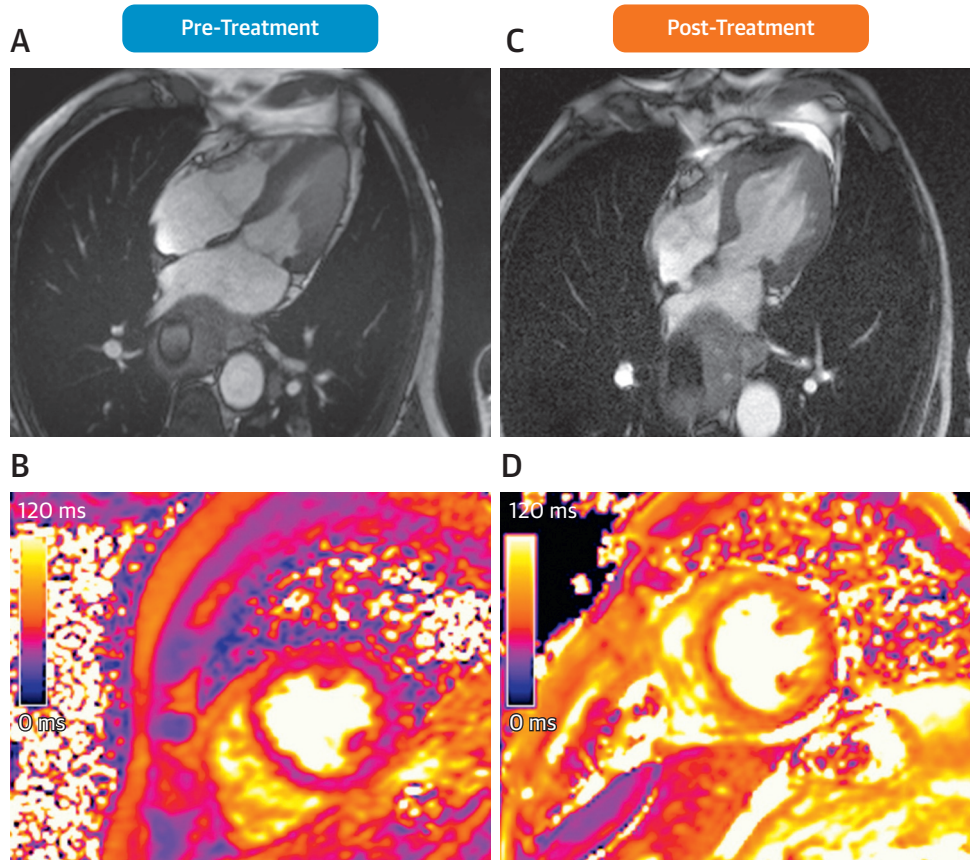
The duration of cancer diagnosis to onset of TLVDS has ranged from <1 to 19 years. TLVDS is associated with cancers of the lung, colorectal system, breast, skin (melanoma), bladder, and hematopoietic system (leukemia) (53–55). A second series of 141 subjects followed across 3 sites in Germany identified similar findings (54). In this particular population, 23.6% of patients experiencing TLVDS also exhibited concomitant cancer diagnoses. Last, 2 cases of TLVDS were associated with exposure to immune checkpoint inhibitors with CMR imaging (56). The second case involved a 77-year-old man with esophageal melanoma who presented with acute heart failure 65 days after beginning immunotherapy with ipilimumab and nivolumab. Imaging patterns of TLVDS in this case (**Figure 4**, Online Videos 5 and 6) included basal and mid-LV akinesis, an LVEF of 40%, absolute GLS of 8.7%, and diffuse myocardial edema identified by elevated T2 mapping values (56). Importantly, no significant corresponding coronary artery luminal narrowings were identified, and LV wall motion abnormalities resolved within 28 days of presentation (56).

At this particular time, the pathophysiological basis for TLVDS in patients with cancer is incompletely understood. In those without cancer, emotional stress has clearly been linked to this syndrome. In patients with cancer, the pathophysiological links are much less certain (53–55). Suggested possible precipitating factors of TLVDS in patients with cancer include a reduction in their susceptibility to perceived stress stimuli and cancer aggravation of cardiac adrenoreceptor sensitivity. It is well known that many patients with cancer experience increased circulating inflammatory mediators, including cytokines, free radicals, and catecholamines, which may heighten adrenoreceptor sensitivity and trigger TLVDS (53–55).

Using magnetic resonance, TLVDS is characterized by regional LV segmental akinesis that most frequently involves the LV apex (**Table 5**). For those patients experiencing recovery of LV systolic function, LGE is often absent (57). In addition to patients with TLVDS experiencing increases in serum troponins, they may or may not experience increased signal on T2-weighted images or increased T2 mapping values (58). These particular imaging findings suggest a transient increase in water uptake within the myocardium that in other disease processes is consistent with an inflammatory condition.

In summary, it is important to recognize that TLVDS occurs in patients with cancer, resulting in LV

FIGURE 4 Cardiovascular Magnetic Resonance Case Example of Transient Left Ventricular Dysfunction Syndrome in Patient With Cancer

Case presentation of a 77-year-old man with esophageal melanoma admitted for acute heart failure with "inverted" transient left ventricular dysfunction syndrome (TLVDS) pattern of basal and mid-left ventricular (LV) akinesia presenting 65 days after treatment with perfusions of ipilimumab and ipilimumab-nivolumab immunotherapy. Pre-treatment cardiovascular magnetic resonance demonstrated normal systolic function (**A**, Online Video 5) and normal T2 signal (36 ms), demonstrating no myocardial edema **(B)**. At 65 days after treatment, his LV ejection fraction (LVEF) was 40% (**C**, Online Video 6), with evidence of myocardial edema by increased T2 signal (mean 60 ms) **(D)**. After treatment with steroids, angiotensin-converting enzyme inhibitors, and beta-blockers, the patient's LVEF returned to 60% within 28 days of initial presentation. Reprinted with permissions from Ederhy et al. (56).

dysfunction and an increase in LV myocardial T2 without LGE. The mechanisms associating TLVDS with cancer are incompletely understood.

Human epidermal growth factor receptor 2 receptor blocker down-regulation of myocardial contractility. Human epidermal growth factor receptor 2 (HER2) overexpression is identified in 25% of all breast cancers (59). Trastuzumab (Herceptin, Genentech, South San Francisco, California) targets the extracellular domain of ErbB2 receptor tyrosine kinase 2 and HER2 and has been shown to interrupt molecular pathways important to cardiovascular health. One proposed mechanism for trastuzumab-associated

LVESV-mediated declines in LVEF involves inhibition of HER2 signaling in cell survival pathways in cardiomyocytes. These pathways inhibit apoptosis and maintain cardiac function and are unable to be

TABLE 5 Key Cardiovascular Magnetic Resonance Features of Stress-Induced Cardiomyopathy

LV segmental akinesis on cine imaging, most frequently involving the apex
Absence of LGE

Abbreviations as in **Table 4**.

TABLE 6 Key Cardiovascular Magnetic Resonance Features of HER2 Receptor Blocker Down-Regulation of Contractility
Decrease in LVEF or myocardial strain with history of trastuzumab treatment
May also have focal LGE
HER2 = human epidermal growth factor receptor 2; other abbreviations as in **Tables 2 and 4**.

TABLE 8 Key Cardiovascular Magnetic Resonance Features of Myocellular Injury
Declines in LVEF or myocardial strain
May also have diffuse LGE or increased T1 or ECV
Abbreviations as in **Tables 1, 4, and 6**.

activated without HER2. A significantly higher risk for cardiac dysfunction occurs in patients who received trastuzumab with anthracyclines (28%) compared with those with anthracyclines alone (10%) (24). Trastuzumab alone has not been found to cause cellular death, is not related to cumulative doses, and is at least partially reversible (60). Early detection of trastuzumab-related cardiac dysfunction is clinically advantageous, as withdrawal or discontinuation and initiation of beta-blockers and angiotensin-converting enzyme inhibitors can reverse the effects (61).

Trastuzumab cardiotoxicity presents along a spectrum from asymptomatic decline in LVEF to symptomatic heart failure (**Table 6**). A study by Fallah-Rad et al. (62) using CMR found that LVEDV and LVESV were increased at 12-month follow-up, with decrease in LVEF from 66 ± 5% to 47 ± 4%. A study by Hare et al. (63) reported slight decreases in longitudinal and radial strain rates after trastuzumab administration, with the earliest changes detected by the longitudinal dimension. For patients with breast cancer receiving anthracycline and trastuzumab, Sawaya et al. (64) found that assessing troponin levels concurrently with peak systolic longitudinal strain imaging after anthracycline exposure improved specificity versus troponin evaluation and strain imaging alone and is useful in the subsequent prediction of cardiotoxicity. In addition, Fallah-Rad et al. (65) observed that LGE using CMR detected early changes in the myocardium due to trastuzumab-related cardiotoxicity, though further study is required.

Trastuzumab cardiotoxicity, or HER2 receptor blocker down-regulation of myocardial contractility,

is related to the immune-mediated destruction of cardiomyocytes caused by binding to the HER2 protein. Monitoring LVEF is the key recommendation from the U.K. National Cancer Research Institute, while evaluating cardiac health, with assessments occurring at baseline, before trastuzumab administration, and 4 and 8 months after treatment (66). Research is ongoing for the predictive value of CMR LGE and longitudinal and radial strain and strain rate as early detectors of cardiac damage (67-71).

Sepsis. Neutropenic fever is a harmful complication associated with the administration of chemotherapy that occurs in up to 5% to 10% of patients with solid tumors, 20% of those with hematologic malignancies, and 70% to 100% of those undergoing bone marrow transplantation (72,73). Among those who develop neutropenic fever, 50% may develop sepsis, with 20% to 30% developing severe and 5% to 10% developing frank septic shock.

To date, relatively few CMR studies have been performed in all comers with sepsis, and there are virtually no reports of CMR in patients with cancer who develop sepsis. In patients with sepsis but without cancer, quantitative myocardial T2 values are elevated (>59 ms), with increased signal intensity on T2-weighted and LGE along the LV epicardial surface with a gradation in signal intensity or T2 values from the epicardial to the endocardial surface (**Table 7**) (74,75). Future studies are needed to describe CMR findings among patients with cancer with sepsis.
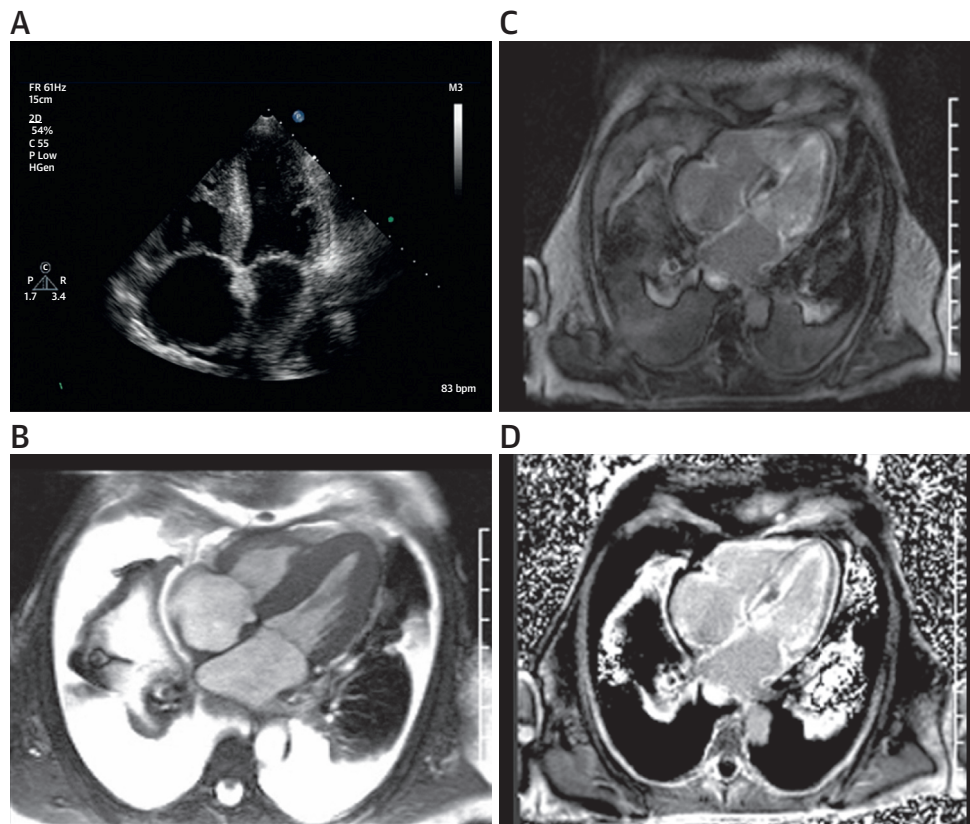
Therapy-related myocellular injury. Patients treated with one of several potentially cardiotoxic cancer therapies are at risk for developing myocellular injury. Anthracyclines are the prototypical agents

TABLE 7 Key Cardiovascular Magnetic Resonance Features of Sepsis
Increased T2w or T2 (>59 ms) and LGE signal intensity with gradation from epicardial to endocardial surface
T2w = T2-weighted; other abbreviations as in **Table 4**.

TABLE 9 Key Cardiovascular Magnetic Resonance Features of Amyloid
Concentric LV wall thickening without myocellular hypertrophy
Subendocardial or diffuse LGE
Elevated native T1 and ECV
Abbreviations as in **Tables 1 and 4**.

FIGURE 5 Case Example of Amyloidosis in Patient With Cancer

Case presentation of a 62-year-old patient with a history of hypertension who presented with a 10-month history of progressive dyspnea, lower extremity edema, elevated serum creatinine of 1.6, and an estimated glomerular filtration rate of 50 ml/min. Still frames from cine 4-chamber echocardiographic and white-blood cardiovascular magnetic resonance images (**A,B**, Online Videos 7 and 8) demonstrating biatrial enlargement and biventricular hypertrophy. Also notable in (**B**) are the presence of extensive pleural and pericardial effusions. Phase-sensitive late gadolinium enhancement magnitude (**C**) and phase-sensitive inversion recovery (**D**) 4-chamber images demonstrate global diffuse and subendocardial enhancement of the left ventricular myocardium typical of cardiac light-chain amyloidosis.

associated with myocellular injury because of: 1) oxidative stress from reactive oxygen and nitrogen species (15,76,77); 2) deoxyribonucleic acid oxidant damage (78); 3) myocellular apoptosis (76,77); and 4) down-regulation of myocellular GATA4 expression (79-81). Topoisomerase-IIβ is also implicated as a mediator of myocellular anthracycline-induced cardiotoxicity (82). In addition to detecting small changes in LVEF related to the administration of
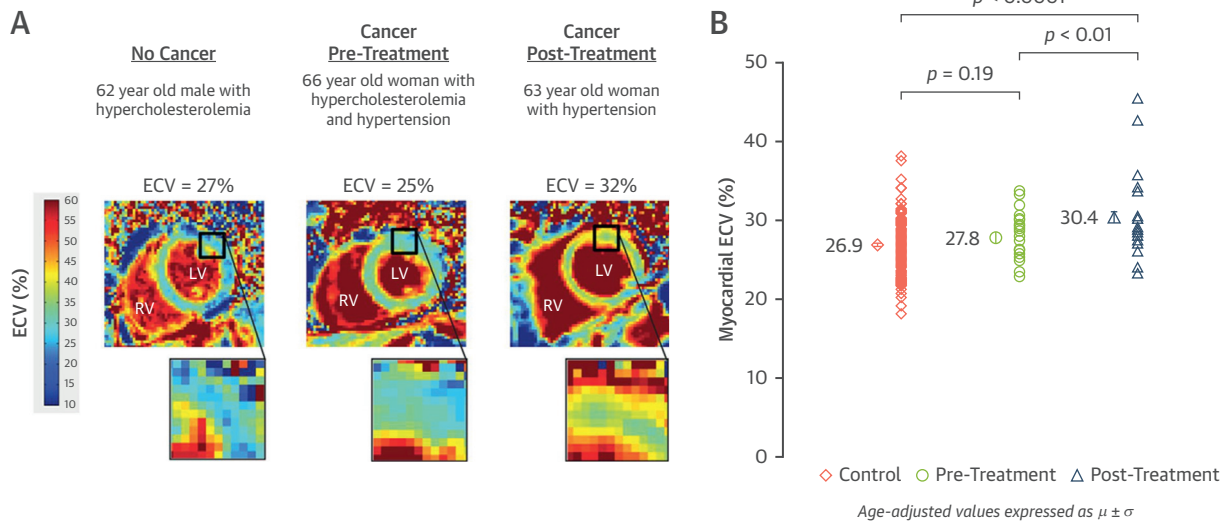
anthracyclines, several studies have investigated the utility of T1-weighted imaging using gadolinium contrast for detecting cardiotoxicity (**Table 8**). In an animal model of cardiotoxicity, Lightfoot et al. (83) demonstrated diffuse LGE with T1-weighted imaging in doxorubicin-treated animals prior to large declines in LVEF. This work was translated by Jordan et al. (84) and demonstrated similar patterns in T1-weighted enhancement in patients treated with anthracycline chemotherapies, with similar observations using quantitative T1 mapping techniques (85).

Mitochondrial dysfunction represents a hallmark of myocellular injury and anthracycline toxicity. CMR research studies are under way to identify

TABLE 10 Key Cardiovascular Magnetic Resonance Features of Iron Overload

Reduced myocardial T2 and T2* values

FIGURE 6 Myocardial Fibrosis Imaging in Anthracycline-Treated Cancer Survivors Using Extracellular Volume Mapping

Case examples demonstrating elevated myocardial fibrosis measured with extracellular volume (ECV) mapping in a cancer survivor **(A)** and aggregated elevations in group data showing mean ECV of 30.4% in anthracycline-treated patients with cancer 3 years after treatment **(B)**. Reprinted with permission from Jordan et al. (100).

changes in bioenergetics and mitochondrial capacity as determinants of fatigability and exercise intolerance using phosphorus spectroscopy in models of heart failure and cardiotoxicity (85,86). Although not ready for clinical use, further research using CMR bioenergetics markers may provide key insights into myocellular injury of current and emerging cancer therapies in research settings.

Factors within the myocardium but extrinsic to the myocyte affecting myocellular contractility. *Infiltrative disorders.* Two infiltrative cardiomyopathies have been more frequently observed in patients with malignancies: amyloid and iron overload. Primary or light-chain amyloidosis is an abnormal accumulation of extracellular protein deposits that when occurring in the myocardium can impair excitation-contraction coupling mechanical dysfunction (87). Primary cardiac amyloid associated with multiple myeloma may present with symptoms of fatigue, signs of weight loss, and a restrictive cardiomyopathy (87–90). Primary cardiac amyloid findings from CMR images include concentric LV wall thickening and increased myocardial tissue volume from amyloid deposition (without myocellular hypertrophy) (**Table 9**). Also, subendocardial or diffuse and patchy LGE (**Figure 5**, Online Videos 7 and 8) may be present. Importantly, tissue characterization with quantitative T1 mapping can differentiate amyloid from noninfiltrative hypertrophy (91). It is important to note that up
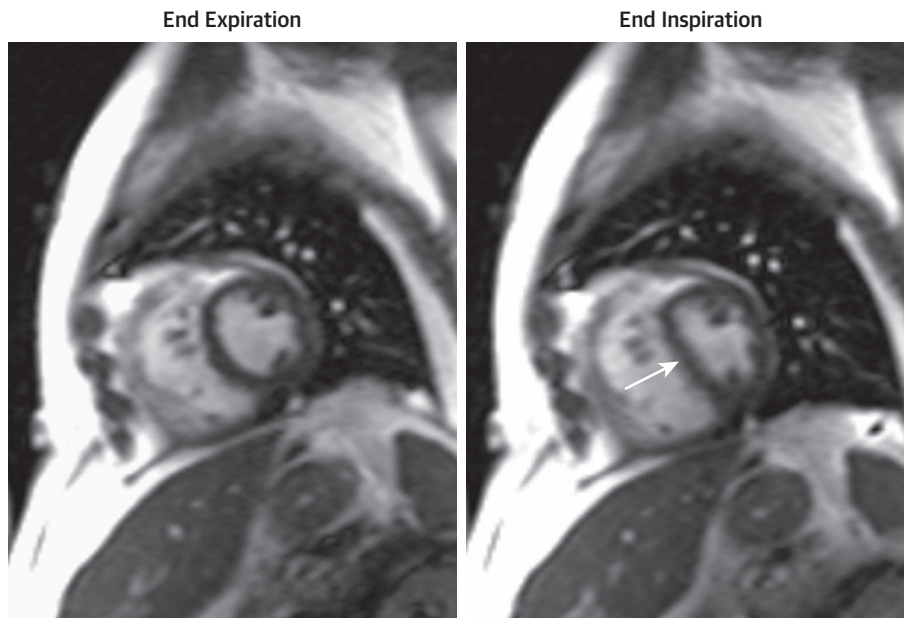
to one-third of patients with amyloidosis may experience 1 of several vascular complications, including intracardiac thrombi or embolic events involving the pulmonic, mesenteric, iliac, brachial, or vascular territory (even in the setting of a preserved LVEF) (92,93). LGE and magnetic resonance angiography (10) may be useful in evaluating these vascular complications.

Iron-overload cardiomyopathy results from iron accumulation in the myocardial tissue and may occur after multiple blood transfusions for aplastic anemia or myelodysplasia (87). This syndrome

TABLE 11 Cardiovascular Magnetic Resonance Imaging Methods to Assess the Right Ventricle in Cardio-Oncology

Right ventricle
Anatomy
Single-phase white-blood imaging in chamber views
Cine white-blood imaging in axial orientation for assessment of RVEDV, RVESV, stroke volume, and RVEF
Function/flow
Cine white-blood imaging in axial orientation for assessment of RVEDV, RVESV, stroke volume, and RVEF
Tissue characterization
Native T1, T2, and T2* mapping
Late gadolinium enhancement imaging
Post-gadolinium contrast-enhanced T1 mapping

RV = right ventricular; RVEDV = right ventricular end-diastolic volume; RVESV = right ventricular end-systolic volume.

FIGURE 7 Cardiovascular Magnetic Resonance Case of Pericardial Constriction in a Patient with Cancer

Case presentation of a 58-year-old man with a history of bone marrow transplantation for acute myelocytic leukemia that presented 7 weeks after sustaining viral pericarditis with lower extremity swelling and fatigue. Cardiovascular magnetic resonance findings suggest constrictive pericardial thickening (5 mm) anterior to the right ventricle. Shown are real-time triggered free-breathing white-blood cine frames at end-expiration **(left)** and end-inspiration **(right)** showing the characteristic septal shift upon inspiration and higher right-sided pressures resulting in a D-shaped left ventricle **(arrow)**. Cine images available as Online Video 9.

also occurs in those with hemochromatosis and hepatocellular cancer who present with a dilated cardiomyopathy (87).

CMR imaging is useful to diagnosis iron-overload cardiomyopathy because T2* characteristics are strongly influenced by the increased accumulation of iron in the LV myocardial tissue, which causes rapid dephasing and signal loss. T2* mapping with CMR should be considered in oncology patients who may have iron-overload cardiomyopathy. Anderson et al. (9) found that a normal myocardial T2* was 52 ± 16 ms, with lower T2* values indicative of increased iron deposition, and furthermore that a T2* <20 ms was associated with progressive and significant decline in systolic function in patients with iron overload (Table 10). Serial examinations with CMR may be used for noninvasive monitoring of resolution of iron overload after treatment.

Interstitial myocardial fibrosis. Myocardial fibrosis due to collagen deposition from acute or chronic disease is associated with several forms of cancer treatment, including the administration of anthracycline chemotherapy, trastuzumab, and radiation therapy (65,94,95). Increases in interstitial fibrosis can impair both LV diastolic and systolic function. Quantitative assessments of interstitial myocardial fibrosis may be assessed using mapping techniques and are noted by increased native T1 and extracellular volume (ECV) fraction measures (7,96). ECV fraction measures are obtained by acquiring T1 assessments before and after GBCA administration and accounting for heart rate and serum hemoglobin (7,96). Anthracycline cardiotoxicity has been associated with diffuse myocardial fibrosis in animal models (97,98) and identified with CMR in cancer survivors and those currently undergoing treatment (94,99,100). Additionally, these patients may have underlying cardiovascular diseases (hypertension, aortic stenosis, diabetes) that also promote diffuse fibrosis, which also may increase myocardial ECV fraction. It is important to understand the shared risk factors between cancer and cardiovascular disease as well as the medical history of an oncology patient when determining if myocardial fibrosis is associated with cancer treatment.

Among 42 adult cancer survivors previously treated with anthracyclines (mean age 55 ± 17 years, 17% treated for breast cancer) undergoing CMR examination for clinical reasons (heart failure or atrial fibrillation) over a median of 89 ± 40 months after receipt of anthracycline-based chemotherapy, LV myocardial ECV fraction was elevated compared with healthy control subjects (36 ± 3% vs. 28 ± 2%, p < 0.0001) (94). Furthermore, the ECV fraction was higher among survivors with reduced LVEFs compared with survivors with preserved LVEFs (38 ± 3% vs. 36 ± 2%, p = 0.03) suggesting that there may be an association between a progressive increase in LV myocardial ECV and LVEF decline after the receipt of anthracycline-based chemotherapy. In studies of asymptomatic pediatric survivors treated with anthracyclines, ECV was not universally elevated above normal values for age, but elevated ECV associations were observed in those with exercise intolerance, prior receipt of high cumulative doses of anthracycline-based chemotherapy, or extensive LV remodeling. Additionally, focal regions of fibrosis were observed in some childhood cancer survivors (95,101). The prognostic significance of these findings is unknown.

More recently, in a cross-sectional analysis of 3 groups of patients—3-year post-anthracycline-treated cancer survivors, newly diagnosed and untreated patients with cancer, and healthy subjects without cancer—native T1 and ECV were higher in previously treated cancer survivors after accounting for demographics, cardiovascular risk factors, and other markers of myocardial remodeling (p < 0.01 for all) (**Figure 6**) (85). Three years after treatment, this study suggests that elevated ECV is associated with prior receipt of anthracycline-based chemotherapy. Future studies are needed to determine whether anthracycline recipients with elevated ECV fraction experience higher rates of cardiovascular events as opposed to cancer survivors.

Additionally, patterns of fibrosis (focal or diffuse) provide strong insight into the origin of underlying disease when quantified or visualized using mapping techniques or LGE imaging (96). Mixed reports of the occurrence and patterns of LGE have been reported among those receiving treatment for breast cancer with anthracyclines, adjuvant trastuzumab, and/or radiotherapy (27,62,65,84,102-105). This is most likely due to the heterogeneity of patient populations and confounding.

Myocardial perfusion deficits. The administration of many cancer therapies, including anthracyclines, 5-fluorouracil, vinblastine, vincristine, and cyclo-

TABLE 12 Cardiovascular Magnetic Resonance Imaging Methods to Assess Pericardial Disease in Cardio-Oncology
Pericardial disease
Anatomy
Dark-blood T1-weighted imaging for anatomy
Fat/water separation imaging to identify pericardium and distinguish from surrounding fat
Function/flow
Cine white-blood imaging (real time) to evaluate function and identify septal shift
Tissue characterization
Fat/water separation imaging to identify pericardium and distinguish from surrounding fat
Late gadolinium enhancement imaging to assess for pericardial tumor invasion

phosphamide, has been shown to injure the vascular endothelium (3,106-108). This injury impairs the endothelial release of nitric oxide to the vascular smooth muscle during times of increased blood flow. Over the long term, a damaged endothelium is susceptible to further injury from accelerated atherosclerosis. The LV perfusion reserve affects the left ventricle's ability to increase the supply of oxygenated blood during stressful periods with increased oxygen demand (such as with exercise).

CMR can perform both quantitative and semiquantitative assessments of myocardial perfusion reserve through contrasted stress examinations with agents such as adenosine (109,110). Patients with cancer may also experience deficits to myocardial perfusion due to aging and atherosclerosis (111,112). At present, CMR perfusion studies have not been performed extensively in patients treated for or surviving cancer.

RIGHT VENTRICULAR DYSFUNCTION

CMR imaging is of particular value relative to other imaging modalities such as echocardiography in the evaluation of suspected right ventricular (RV) dysfunction in patients with cancer. RV dysfunction in patients with cancer or surviving cancer may be due to primary or metastatic neoplasms or secondary to chemotherapy (14). Imaging of RV dysfunction primarily involves cine white-blood imaging in the axial and sagittal planes for assessment of volumes and ejection fraction (**Table 11**). Although tissue characterization techniques may be possible in some situations, they may suffer from inadequate spatial resolution due to the relatively thin wall of the right ventricle.

Most studies describing RV dysfunction in patients with cancer involve survivors of pediatric

cancers and malignancies who were treated with anthracycline-based chemotherapy. In a study of 62 pediatric survivors (mean age at CMR 14.6 years, ≥5 years post-treatment), 80% of participants demonstrated either abnormal or subnormal RV ejection fraction (RVEF): 27% and 53%, respectively (113). Similar findings of impairment in RVEF have been observed in pediatric survivors late after cancer treatment in which RVEF averaged <50% in the studied population (114). More recently in a study of 41 adult patients with breast cancer treated with trastuzumab, transient changes in RV function were observed prospectively with CMR. Compared with baseline, RVEFs were reduced at 6 and 12 months after initiating trastuzumab with near resolution at the 18-month CMR examination (115). In this study, the changes in RVEF occurred independent of changes in LVEF (115) and demonstrate the utility of CMR examinations to identify RV dysfunction in patients with cancer. The prognostic importance of RV dysfunction in patients with cancer is unknown.

ANTHRACYCLINE-ASSOCIATED DECLINES IN LV MASS

Increasingly it is recognized that prior anthracycline exposure is associated with future declines in LV mass. Potential etiologies for this decline include myocellular injury or death with or without the occurrence of intracellular fibrosis, or myocardial progenitor cell population depletion (27). CMR can quantify LV mass in an accurate, reproducible manner implementing 1 of several 3D image acquisition strategies that involve a modified Simpson's rule method of analysis (10).

Among 91 long-term cancer survivors who received anthracyclines, adverse cardiovascular events occurred more frequently in those receiving higher doses of anthracyclines during treatment and who subsequently developed larger declines in LV mass (103). In multivariate analysis, LV mass was the strongest predictor of admission for decompensated heart failure, implantable cardiovascular defibrillator therapy, or cardiovascular death (p < 0.001) (103). In a second study of 61 patients undergoing anthracycline chemotherapy, declines in LV mass, and not LVEF, 6 months after initiating chemotherapy were independently associated with worsening heart failure (116). Results from studies such as this suggest that further research should be performed to investigate the impact of potential cardiotoxic chemotherapy on LV mass. CMR may have an important role in this research, as with tissue characterization techniques,

TABLE 13 Cardiovascular Magnetic Resonance Imaging Methods to Assess the Valve Leaflets in Cardio-Oncology
Valve leaflets
Anatomy
Dark-blood T1-weighted imaging for anatomy
Function/flow
Cine white-blood imaging
Phase-contrast assessment of valvular regurgitation or stenosis
Tissue characterization
Native T1 and T2 mapping
Late gadolinium enhancement imaging of valve mass with and without prolonged inversion time

one may be able to differentiate the etiology of LV mass declines (e.g., myocellular injury, decreases in myocellular size [117], or changes in the amount of interstitial fibrosis relative to myocyte number or size).

ADDITIONAL CMR EVALUATIONS IN PATIENTS WITH CANCER

It is important to recognize that CMR may be useful to assess conditions other than those that are necessarily related to LV or RV myocardial contractility or relaxation. These additional evaluations include assessment of pericardial disease and valvular disease or identification of myocardial masses.
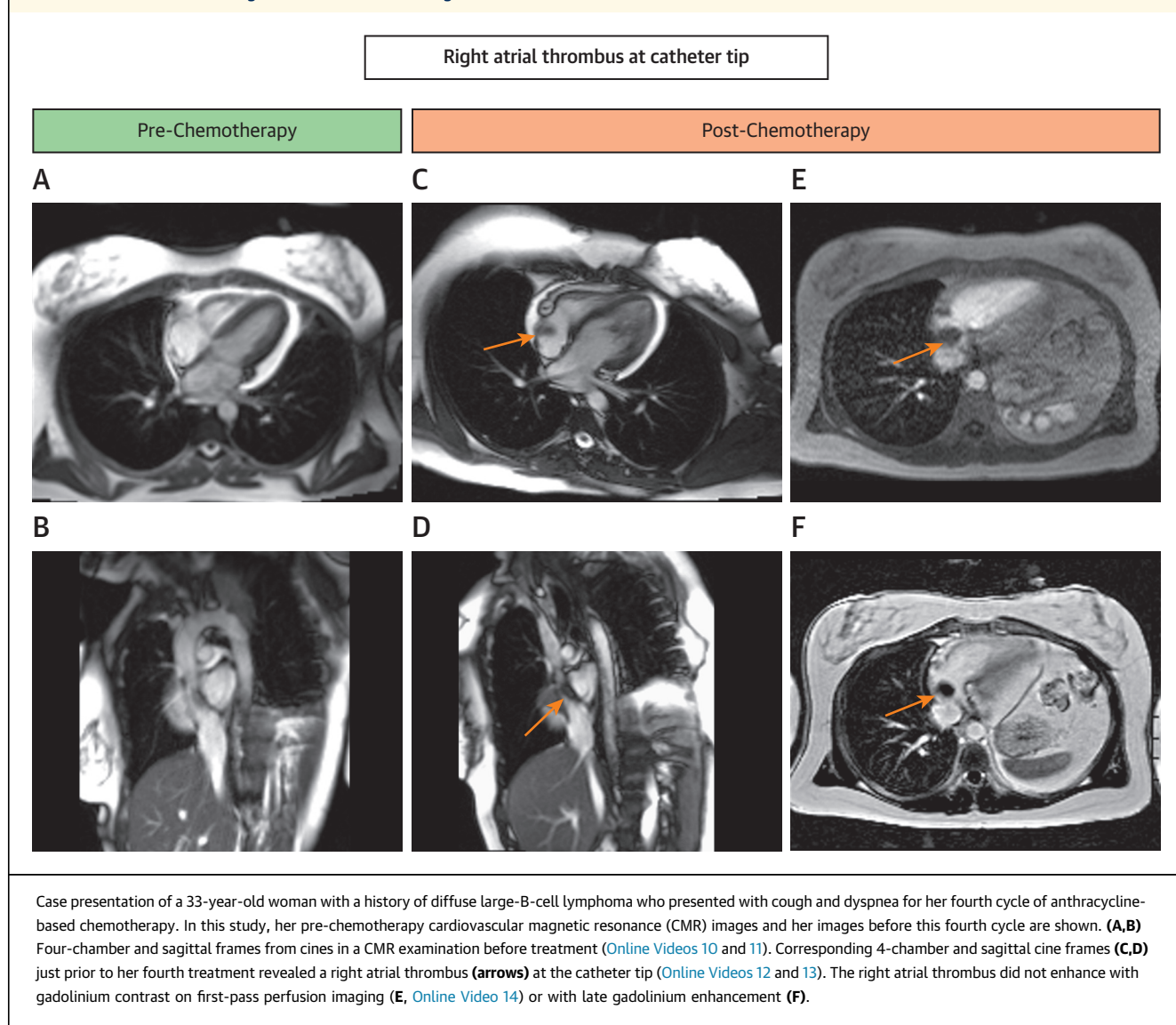
PERICARDIAL DISEASE ASSESSMENT. There are 3 primary considerations for using CMR to evaluate pericardial disease among patients with or receiving treatment for cancer: 1) tumor invasion of the parietal or visceral pericardium that may or may not be complicated by the concomitant presence of a pericardial effusion; 2) the development of pericardial inflammation or pericarditis; and 3) evaluation or exclusion of pericardial constriction (e.g., after external beam radiation) (118-121).

TABLE 14 Cardiovascular Magnetic Resonance Imaging Methods to Assess Cardiac Masses in Cardio-Oncology
Cardiac Masses
Anatomy
Dark-blood T1-weighted imaging with and without fat saturation
Function/flow
Cine white-blood imaging
Tissue characterization
Native T1, T2, and T2* mapping in at least 2 orthogonal planes
Gadolinium-enhanced T1-weighted first-pass perfusion imaging
Late gadolinium enhancement of mass with and without prolonged inversion time
Post-gadolinium contrast-enhanced T1 mapping

FIGURE 8   Cardiovascular Magnetic Resonance Case of Right Atrial Thrombus

Right atrial thrombus at catheter tip

Pre-Chemotherapy	Post-Chemotherapy

Case presentation of a 33-year-old woman with a history of diffuse large-B-cell lymphoma who presented with cough and dyspnea for her fourth cycle of anthracycline-based chemotherapy. In this study, her pre-chemotherapy cardiovascular magnetic resonance (CMR) images and her images before this fourth cycle are shown. **(A,B)** Four-chamber and sagittal frames from cines in a CMR examination before treatment (Online Videos 10 and 11). Corresponding 4-chamber and sagittal cine frames **(C,D)** just prior to her fourth treatment revealed a right atrial thrombus **(arrows)** at the catheter tip (Online Videos 12 and 13). The right atrial thrombus did not enhance with gadolinium contrast on first-pass perfusion imaging **(E,** Online Video 14) or with late gadolinium enhancement **(F)**.

To identify either of these processes, dark-blood structural and cine white-blood functional imaging is often implemented to visualize the pericardial space and the effects of respiration on RV and LV septal motion and systolic and diastolic function (Figure 7, Online Video 9, Table 12). These pieces of information are very useful for identifying hemodynamic consequences associated with pericardial tamponade or constriction (118-122).

The application of myocardial tagging techniques may be used to confirm adherence of the visceral to the parietal pericardium in patients with limited cardiac contraction and relaxation due to pericardial constriction. Additionally, T1 and T2 mapping

methodologies may facilitate identification of hemorrhagic versus nonhemorrhagic effusions. This latter feature is valuable when evaluating malignant pericardial effusions due to metastatic cancer from the breast, lung, or lymphatic system.
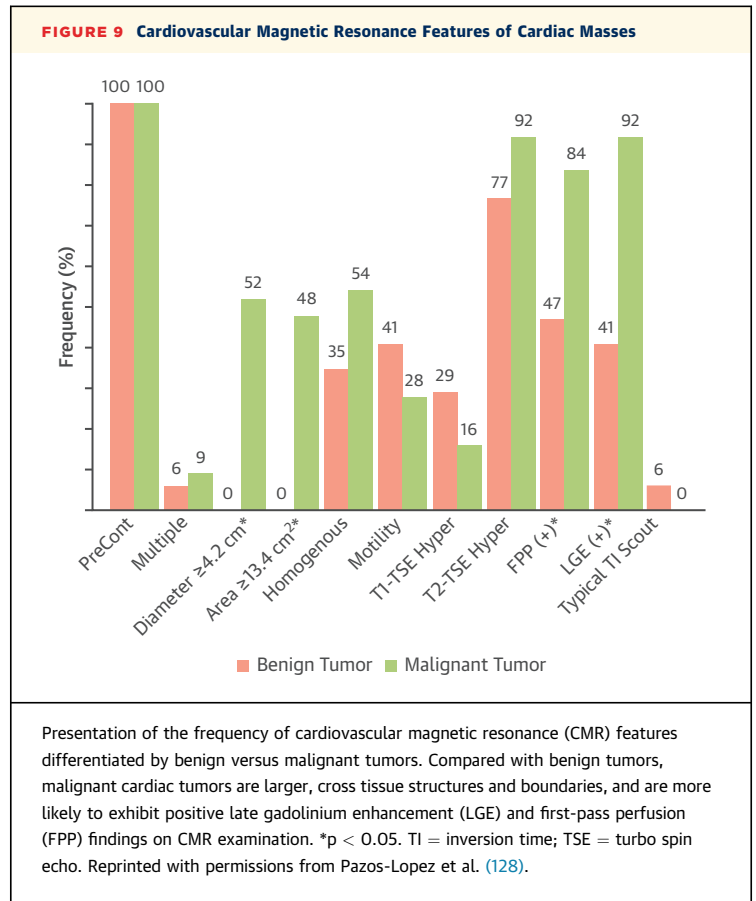
Both T1 mapping and coordination of T1-weighted imaging with the first-pass arrival of gadolinium contrast into both the myocardium and pericardial space can help differentiate invasive tumors from other structures within the pericardial space (118-122). Differentiating pericardial inflammation from fibrosis in the presence of pericarditis is difficult, even with CMR imaging. It has been shown, however, that pericardial LGE is most

frequently associated with pericardial inflammation (123), whereas end-stage or chronic fibrotic constrictive pericarditis does not enhance after contrast but may show morphologic findings of constriction (124).

EVALUATION OF VALVE LEAFLETS. Transthoracic and transesophageal echocardiography are the most widely used imaging methodologies used to identify heart valve-related abnormalities (125). In patients with cancer who may also experience valvular heart disease, CMR has an American College of Cardiology/ American Heart Association Class I indication for assessing the severity of mitral and aortic regurgitation or aortic stenosis, particularly when echocardiographic assessments are inadequate or uncertain (126). Valvular stenosis or regurgitation may arise as a complication of primary invasion of a tumor into the valve apparatus or after the administration of radiation therapy and can be appreciated with CMR (**Table 13**). In addition to these indications, CMR may be helpful to assess the etiology of masses on the valve leaflets themselves, as described further in the next section.

IDENTIFICATION OF CARDIAC MASSES AND TUMORS. CMR evaluation of cardiac and extracardiac masses is helpful for identifying primary cardiac tumors, metastatic foci, thrombi, and infectious abscesses (127). When performing a CMR study to assess cardiac masses, one can locate determine the etiology and assess the functional importance of the mass on cardiac performance (128,129). Visualizing and comparing the behavior of voxels within the mass with these various imaging techniques allows the differentiation of cardiac tumors from thrombi (127–131).

Masses are identified with both dark- and white-blood imaging methods followed by cine gradient-echo or steady-state free precision imaging to assess functional importance (**Table 14**) (129). After locating the mass, a combination of T1-, T2-, and T2*-weighted images with or without selective hydrogen imaging (fat or water saturation), and in some cases gadolinium contrast (assessing early and late enhancement), is performed (128). Pazos-Lopez et al. (128) and Caspar et al. (127) provided detailed reviews of CMR differentiation among thrombi, benign masses, and malignant masses. Briefly, compared with thrombi, cardiac tumors are larger in size, demonstrate heterogeneous tissue composition, and show a higher frequency of first-pass perfusion and LGE because of vascularity and contrast uptake (128). A right atrial thrombus from a

FIGURE 9 Cardiovascular Magnetic Resonance Features of Cardiac Masses

Presentation of the frequency of cardiovascular magnetic resonance (CMR) features differentiated by benign versus malignant tumors. Compared with benign tumors, malignant cardiac tumors are larger, cross tissue structures and boundaries, and are more likely to exhibit positive late gadolinium enhancement (LGE) and first-pass perfusion (FPP) findings on CMR examination. *p < 0.05. TI = inversion time; TSE = turbo spin echo. Reprinted with permissions from Pazos-Lopez et al. (128).

catheter tip in a patient receiving chemotherapy is shown in **Figure 8** and Online Videos 10, 11, 12, 13, and 14. Compared with benign tumors, malignant cardiac tumors are larger, cross tissue structures and boundaries, and are more likely to have positive LGE and first-pass perfusion findings on CMR examination (**Figure 9**) (128).

FUTURE DIRECTIONS

Moving forward, there are several unanswered questions in the emerging field of cardio-oncology for which CMR may play an important role. First, it is increasingly recognized that exercise intolerance and fatigue contribute to cardiovascular morbidity among those with or surviving cancer (132,133). For many years, it was believed that reductions in exercise-associated cardiac output due to diminished LV performance were the primary contributor to decreased exercise capacity in those treated for cancer (134). However, recent data suggest that reductions in exercise-associated arteriovenous oxygen difference may also contribute to the reduction in exercise

capacity (135). This abnormality may result from vascular or skeletal muscle injury due to cancer treatments or overall inactivity while receiving cancer therapy. The utility of CMR exercise protocols in which both resting and exercise-associated cardiac output and arteriovenous oxygen difference measurements may facilitate understanding the etiology of exercise intolerance and fatigue in patients with and surviving cancer (136).

Second, several cancer therapeutic agents (e.g., anthracyclines) are known to inflict mitochondrial injury in the cardiomyocyte. Two opportunities exist with CMR to investigate their function. One involves using multinuclear phosphorus spectroscopy to assess myocardial adenosine triphosphate/phosphocreatine ratio as a measure of bioenergetics in the heart (137). The second opportunity involves similar phosphorus bioenergetic assessments in the skeletal muscle (138). Perhaps disorders of skeletal muscle energetics could be contributing to exercise intolerance experienced by patients with cancer.

Third, it is increasingly recognized that many patients treated for cancer experience cognitive dysfunction (139). At present, the mechanism of cognitive decline in patients with cancer is not well described. In other disease processes, the combination of cardiac large-vessel (aorta) and cerebral microcirculatory and central nervous system structural imaging has been implemented to identify large- and small-vessel vascular disorders associated with cognitive decline (140). As yet, these techniques have not been implemented in patients with cancer. Investigations using these techniques may provide insight into the cognitive decline observed in patients with cancer.

Finally, CMR measures have not been readily adopted into position or guideline statements related to the management of patients receiving potentially cardiotoxic or renovascular-toxic cancer treatments.

As CMR-derived measures of myocardial mass, mapping, and vascular function become more widespread, research to determine the optimal incorporation of these measures into statements related to management of patients with cancer are warranted.

CONCLUSIONS

An increasing number of patients with or receiving treatment for cancer or malignancies are at increased risk for cardiovascular events during and after treatment involving a spectrum of conditions. This includes subclinical and overt clinical cardiovascular disease involving the pericardium or the heart itself. Through the assessment of cardiac anatomy, function, blood flow, T1 and T2 mapping, or 1 of several gadolinium-based tissue characterization techniques, CMR is proving useful to noninvasively assess and characterize the extent and severity of these cardiac abnormalities. The information provided by CMR offers the opportunity to institute therapy that maximizes cardiovascular performance and thereby enable reductions in the overall morbidity experienced by patients with cancer. In addition, new research opportunities exist with CMR that may provide information pertaining to the mechanisms by which exercise intolerance and cognitive dysfunction are related to cancer therapeutics. Additional research will be helpful to determine how to best integrate CMR measures into guidelines used to direct therapy to preserve cardiovascular function in patients with or receiving treatment for cancer.

ADDRESS FOR CORRESPONDENCE: Dr. Jennifer H. Jordan, Wake Forest University Health Sciences, Bowman Gray Campus, Medical Center Boulevard, Winston-Salem, North Carolina 27157-1045. E-mail: jennifer.jordan@wakehealth.edu. Twitter: @JenJordanPhD.

REFERENCES

1. Barac A, Murtagh G, Carver JR, et al. Cardiovascular health of patients with cancer and cancer survivors: a roadmap to the next level. J Am Coll Cardiol 2015;65:2739–46.

2. Mulrooney DA, Yeazel MW, Kawashima T, et al. Cardiac outcomes in a cohort of adult survivors of childhood and adolescent cancer: retrospective analysis of the Childhood Cancer Survivor Study cohort. BMJ 2009;339:b4606.

3. Vasu S, Hundley WG. Understanding cardiovascular injury after treatment for cancer: an overview of current uses and future directions of cardiovascular magnetic resonance. J Cardiovasc Magn Reson 2013;15:66–83.

4. Kongbundansuk S, Hundley WG. Noninvasive imaging of cardiovascular injury related to the treatment of cancer. J Am Coll Cardiol Img 2014;7:824–38.

5. Thavendiranathan P, Grant AD, Negishi T, Plana JC, Popovic ZB, Marwick TH. Reproducibility of echocardiographic techniques for sequential assessment of left ventricular ejection fraction and volumes: application to patients undergoing cancer chemotherapy. J Am Coll Cardiol 2013;61:77-84.

6. Friedrich MG, Sechtem U, Schulz-Menger J, et al. Cardiovascular magnetic resonance in myocarditis: a JACC white paper. J Am Coll Cardiol 2009;53:1475–87.

7. Moon JC, Messroghli DR, Kellman P, et al. Myocardial T1 mapping and extracellular volume quantification: a Society for Cardiovascular Magnetic Resonance (SCMR) and CMR Working Group of the European Society of Cardiology consensus statement. J Cardiovasc Magn Reson 2013;15:92.

8. Schulz-Menger J, Bluemke DA, Bremerich J, et al. Standardized image interpretation and post processing in cardiovascular magnetic resonance:

Society for Cardiovascular Magnetic Resonance (SCMR) Board of Trustees Task Force on Standardized Post Processing. J Cardiovasc Magn Reson 2013;15:35–53.

9. Anderson L, Holden S, Davis B, et al. Cardiovascular T2-star (T2*) magnetic resonance for the early diagnosis of myocardial iron overload. Eur Heart J 2001;22:2171–9.

10. Hundley WG, Bluemke DA, Finn JP, et al. ACCF/ACR/AHA/NASCI/SCMR 2010 expert consensus document on cardiovascular magnetic resonance: a report of the American College of Cardiology Foundation Task Force on Expert Consensus Documents. J Am Coll Cardiol 2010;55:2614–62.

11. McDonald RJ, McDonald JS, Kallmes DF, et al. Intracranial gadolinium deposition after contrast-enhanced MR imaging. Radiology 2015;275:772–82.

12. Murata N, Gonzalez-Cuyar LF, Murata K, et al. Macrocyclic and other non-group 1 gadolinium contrast agents deposit low levels of gadolinium in brain and bone tissue: preliminary results from 9 patients with normal renal function. Invest Radiol 2016;51:447–53.

13. Montagne A, Toga AW, Zlokovic BV. Blood-brain barrier permeability and gadolinium: benefits and potential pitfalls in research. JAMA Neurol 2016;73:13–4.

14. Plana JC, Galderisi M, Barac A, et al. Expert consensus for multimodality imaging evaluation of adult patients during and after cancer therapy: a report from the American Society of Echocardiography and the European Association of Cardiovascular Imaging. J Am Soc Echocardiogr 2014;27:911–39.

15. Ewer MS, Yeh ET. Cancer and the heart. Raleigh, North Carolina: PMPH-USA; 2013.

16. Schwartz RG, McKenzie WB, Alexander J, et al. Congestive heart failure and left ventricular dysfunction complicating doxorubicin therapy. Seven-year experience using serial radionuclide angiocardiography. Am J Med 1987;82:1109–18.

17. Walker J, Bhullar N, Fallah-Rad N, et al. Role of three-dimensional echocardiography in breast cancer: comparison with two-dimensional echocardiography, multiple-gated acquisition scans, and cardiac magnetic resonance imaging. J Clin Oncol 2010;28:3429–36.

18. Cardinale D, Colombo A, Bacchiani G, et al. Early detection of anthracycline cardiotoxicity and improvement with heart failure therapy. Circulation 2015;131:1981–8.

19. Hundley WG, Bluemke DA, Finn JP, et al. ACCF/ACR/AHA/NASCI/SCMR 2010 expert consensus document on cardiovascular magnetic resonance: a report of the American College of Cardiology Foundation Task Force on Expert Consensus Documents. J Am Coll Cardiol 2010;55:2614–62.

20. Bellenger N, Burgess M, Ray S, et al. Comparison of left ventricular ejection fraction and volumes in heart failure by echocardiography, radionuclide ventriculography and cardiovascular magnetic resonance. Are they interchangeable? Eur Heart J 2000;21:1387–96.

21. Raman SV, Shah M, McCarthy B, Garcia A, Ferketich AK. Multi-detector row cardiac computed tomography accurately quantifies right and left ventricular size and function compared with cardiac magnetic resonance. Am Heart J 2006;151:736–44.

22. Alexander J, Dainiak N, Berger HJ, et al. Serial assessment of doxorubicin cardiotoxicity with quantitative radionuclide angiocardiography. N Engl J Med 1979;300:278–83.

23. Walker CM, Saldana DA, Gladish GW, et al. Cardiac complications of oncologic therapy. Radiographics 2013;33:1801–15.

24. Panjrath GS, Jain D. Trastuzumab-induced cardiac dysfunction. Nucl Med Commun 2007;28:69–73.

25. Hall PS, Harshman LC, Srinivas S, Witteles RM. The frequency and severity of cardiovascular toxicity from targeted therapy in advanced renal cell carcinoma patients. J Am Coll Cardiol HF 2013;1:72–8.

26. Wassmuth R, Lentzsch S, Erdbruegger U, et al. Subclinical cardiotoxic effects of anthracyclines as assessed by magnetic resonance imaging—a pilot study. Am Heart J 2001;141:1007–13.

27. Drafts BC, Twomley KM, D'Agostino R Jr., et al. Low to moderate dose anthracycline-based chemotherapy is associated with early noninvasive imaging evidence of subclinical cardiovascular disease. J Am Coll Cardiol Img 2013;6:877–85.

28. Armstrong GT, Plana JC, Zhang N, et al. Screening adult survivors of childhood cancer for cardiomyopathy: comparison of echocardiography and cardiac magnetic resonance imaging. J Clin Oncol 2012;30:2876.

29. Wang K, Eblan MJ, Deal AM, et al. Cardiac toxicity after radiotherapy for stage III non-small-cell lung cancer: pooled analysis of dose-escalation trials delivering 70 to 90 Gy. J Clin Oncol 2017;35:1387–94.

30. Adams MJ, Hardenbergh PH, Constine LS, Lipshultz SE. Radiation-associated cardiovascular disease. Crit Rev Oncol Hematol 2003;45:55–75.

31. Ewer MS, Ali MK, Mackay B, et al. A comparison of cardiac biopsy grades and ejection fraction estimations in patients receiving Adriamycin. J Clin Oncol 1984;2:112–7.

32. Thavendiranathan P, Poulin F, Lim K-D, Plana JC, Woo A, Marwick TH. Use of myocardial strain imaging by echocardiography for the early detection of cardiotoxicity in patients during and after cancer chemotherapy: a systematic review. J Am Coll Cardiol 2014;63:2751–68.

33. Romano S, Judd RM, Kim RJ, et al. Association of feature-tracking cardiac magnetic resonance imaging left ventricular global longitudinal strain with all-cause mortality in patients with reduced left ventricular ejection fraction. Circulation 2017;135:2313–5.

34. Jolly M-P, Jordan JH, Meléndez GC, McNeal GR, D'Agostino RB, Hundley WG. Automated assessments of circumferential strain from cine CMR correlate with LVEF declines in cancer patients early after receipt of cardio-toxic chemotherapy. J Cardiovasc Magn Reson 2017;19:59.

35. Aletras AH, Ding SJ, Balaban RS, Wen H. DENSE: displacement encoding with stimulated echoes in cardiac functional MRI. J Magn Reson 1999;137:247–52.

36. Osman NF, Kerwin WS, McVeigh ER, Prince JL. Cardiac motion tracking using CINE harmonic phase (HARP) magnetic resonance imaging. Magn Reson Med 1999;42:1048–60.

37. Meléndez GC, Sukpraphrute B, D'Agostino RB, et al. Frequency of left ventricular end-diastolic volume-mediated declines in ejection fraction in patients receiving potentially cardiotoxic cancer treatment. Am J Cardiol 2017;119:1637–42.

38. Jordan JH, Sukpraphrute B, Meléndez GC, Jolly M-P, D'Agostino RB, Hundley WG. Early myocardial strain changes during potentially cardiotoxic chemotherapy may occur as a result of reductions in left ventricular end-diastolic volume. Circulation 2017;135:2575–7.

39. Belmonte F, Das S, Sysa-Shah P, et al. ErbB2 overexpression upregulates antioxidant enzymes, reduces basal levels of reactive oxygen species, and protects against doxorubicin cardiotoxicity. Am J Physiol Heart Circ Physiol 2015;309:H1271–80.

40. Li W, Croce K, Steensma DP, McDermott DF, Ben-Yehuda O, Moslehi J. Vascular and metabolic implications of novel targeted cancer therapies: focus on kinase inhibitors. J Am Coll Cardiol 2015;66:1160–78.

41. Kawel-Boehm N, Maceira A, Valsangiacomo-Buechel ER, et al. Normal values for cardiovascular magnetic resonance in adults and children. J Cardiovasc Magn Reson 2015;17:29.

42. Benetos A, Waeber B, Izzo J, et al. Influence of age, risk factors, and cardiovascular and renal disease on arterial stiffness: clinical applications. Am J Hypertens 2002;15:1101–8.

43. Chaosuwannakit N, D'Agostino R Jr., Hamilton CA, et al. Aortic stiffness increases upon receipt of anthracycline chemotherapy. J Clin Oncol 2010;28:166–72.

44. Grover S, Lou PW, Bradbrook C, et al. Early and late changes in markers of aortic stiffness with breast cancer therapy. Intern Med J 2015;45:140–7.

45. Wang DY, Okoye GD, Neilan TG, Johnson DB, Moslehi JJ. Cardiovascular toxicities associated with cancer immunotherapies. Curr Cardiol Rep 2017;19:21.

46. Liu PP, Mason JW. Advances in the understanding of myocarditis. Circulation 2001;104:1076–82.

47. Moslehi JJ. Cardiovascular toxic effects of targeted cancer therapies. N Engl J Med 2016;375:1457–67.

48. Johnson DB, Balko JM, Compton ML, et al. Fulminant myocarditis with combination immune checkpoint blockade. N Engl J Med 2016;375:1749–55.

49. Mahrholdt H, Goedecke C, Wagner A, et al. Cardiovascular magnetic resonance assessment of human myocarditis: a comparison to histology and molecular pathology. Circulation 2004;109:1250–8.

50. Mahrholdt H, Wagner A, Judd RM, Sechtem U. Assessment of myocardial viability by cardiovascular magnetic resonance imaging. Eur Heart J 2002;23:602–19.

51. Kindermann I, Barth C, Mahfoud F, et al. Update on myocarditis. J Am Coll Cardiol 2012;59:779–92.

52. Mahmood SS, Fradley MG, Cohen JV, et al. Myocarditis in patients treated with immune checkpoint inhibitors. J Am Coll Cardiol 2018;71:1755–64.

53. Burgdorf C, Kurowski V, Radke PW. Long-term prognosis of transient left ventricular ballooning syndrome and cancer. Heart Lung 2011;40:472.

54. Burgdorf C, Nef HM, Haghi D, Kurowski V, Radke PW. Tako-tsubo (stress-induced) cardiomyopathy and cancer. Ann Intern Med 2010;152:830–1.

55. Burgdorf C, Kurowski V, Bonnemeier H, Schunkert H, Radke PW. Long-term prognosis of the transient left ventricular dysfunction syndrome (tako-tsubo cardiomyopathy): focus on malignancies. Eur J Heart Fail 2008;10:1015–9.

56. Ederhy S, Cautela J, Ancedy Y, Escudier M, Thuny F, Cohen A. Takotsubo-like syndrome in cancer patients treated with immune checkpoint inhibitors. J Am Coll Cardiol Img 2018;11:1187–90.

57. Leurent G, Larralde A, Boulmier D, et al. Cardiac MRI studies of transient left ventricular apical ballooning syndrome (takotsubo cardiomyopathy): a systematic review. Int J Cardiol 2009;135:146–9.

58. Neil C, Nguyen TH, Kucia A, et al. Slowly resolving global myocardial inflammation/oedema in tako-tsubo cardiomyopathy: evidence from T2-weighted cardiac MRI. Heart 2012;98:1278–84.

59. Bilous M, Ades C, Armes J, et al. Predicting the HER2 status of breast cancer from basic histopathology data: an analysis of 1500 breast cancers as part of the HER2000 International Study. Breast 2003;12:92–8.

60. Ewer SM, Ewer MS. Cardiotoxicity profile of trastuzumab. Drug Saf 2008;31:459–67.

61. Onitilo AA, Engel JM, Stankowski RV. Cardiovascular toxicity associated with adjuvant trastuzumab therapy: prevalence, patient characteristics, and risk factors. Ther Adv Drug Saf 2014;5:154–66.

62. Fallah-Rad N, Walker JR, Wassef A, et al. The utility of cardiac biomarkers, tissue velocity and strain imaging, and cardiac magnetic resonance imaging in predicting early left ventricular dysfunction in patients with human epidermal growth factor receptor II-positive breast cancer treated with adjuvant trastuzumab therapy. J Am Coll Cardiol 2011;57:2263–70.

63. Hare JL, Brown JK, Leano R, Jenkins C, Woodward N, Marwick TH. Use of myocardial deformation imaging to detect preclinical myocardial dysfunction before conventional measures in patients undergoing breast cancer treatment with trastuzumab. Am Heart J 2009;158:294–301.

64. Sawaya H, Sebag IA, Plana JC, et al. Assessment of echocardiography and biomarkers for the extended prediction of cardiotoxicity in patients treated with anthracyclines, taxanes, and trastuzumab. Circ Cardiovasc Imag 2012;5:596–603.

65. Fallah-Rad N, Lytwyn M, Fang TL, Kirkpatrick I, Jassal DS. Delayed contrast enhancement cardiac magnetic resonance imaging in trastuzumab induced cardiomyopathy. J Cardiovasc Magn Reson 2008;10:5.

66. Jones AL, Barlow M, Barrett-Lee PJ, et al. Management of cardiac health in trastuzumab-treated patients with breast cancer: updated United Kingdom National Cancer Research Institute recommendations for monitoring. Br J Cancer 2009;100:684–92.

67. A Prospective Study of Breast Cancer Patients with Abnormal Strain Imaging. Available at: https://clinicaltrials.gov/ct2/show/NCT02993198. Accessed June 30, 2018.

68. Strain Imaging in Breast Cancer Patients Receiving Trastuzumab. Available at: https://clinicaltrials.gov/ct2/show/NCT02080390. Accessed June 30, 2018.

69. Carvedilol for the Prevention of Anthracycline/Anti-HER2 Therapy Associated Cardiotoxicity Among Women With HER2-Positive Breast Cancer Using Myocardial Strain Imaging for Early Risk Stratification. Available at: https://clinicaltrials.gov/ct2/show/NCT02177175. Accessed June 30, 2018.

70. Assessment for Long-Term Cardiovascular Impairment Associated With Trastuzumab Cardiotoxicity in HER2-Positive Breast Cancer Survivors. Available at: https://clinicaltrials.gov/ct2/show/NCT02615054. Accessed June 30, 2018.

71. Evaluation of Myocardial Changes During Breast Adenocarcinoma Therapy to Detect Cardiotoxicity Earlier With MRI (EMBRACE-MRI). Available at: https://clinicaltrials.gov/ct2/show/NCT02306538. Accessed June 30, 2018.

72. Culakova E, Thota R, Poniewierski MS, et al. Patterns of chemotherapy-associated toxicity and supportive care in US oncology practice: a nationwide prospective cohort study. Cancer Med 2014;3:434–44.

73. Thursky KA, Worth LJ. Can mortality of cancer patients with fever and neutropenia be improved? Curr Opin Infect Dis 2015;28:505–13.

74. De Lazzari M, Marra MP, Cacciavillani L, et al. Inside myocardial dysfunction in septic shock: mechanism of troponin release highlighted by cardiac magnetic resonance. J Cardiovasc Med (Hagerstown) 2017;18:818–9.

75. Siddiqui Y, Crouser ED, Raman SV. Non-ischemic myocardial changes detected by cardiac magnetic resonance in critical care patients with sepsis. Am J Respir Crit Care Med 2013;188:1037–9.

76. Childs AC, Phaneuf SL, Dirks AJ, Phillips T, Leeuwenburgh C. Doxorubicin treatment in vivo causes cytochrome C release and cardiomyocyte apoptosis, as well as increased mitochondrial efficiency, superoxide dismutase activity, and Bcl-2: Bax ratio. Cancer Res 2002;62:4592–8.

77. An J, Li P, Li J, Dietz R, Donath S. ARC is a critical cardiomyocyte survival switch in doxorubicin cardiotoxicity. J Mol Med (Berl) 2009;87:401–10.

78. Sorensen BS, Sinding J, Andersen AH, Alsner J, Jensen PB, Westergaard O. Mode of action of topoisomerase II-targeting agents at a specific DNA sequence: uncoupling the DNA binding, cleavage and religation events. J Mol Biol 1992;228:778–86.

79. Kim Y, Ma AG, Kitta K, et al. Anthracycline-induced suppression of GATA-4 transcription factor: implication in the regulation of cardiac myocyte apoptosis. Mol Pharmacol 2003;63:368–77.

80. Zhu S-G, Kukreja RC, Das A, Chen Q, Lesnefsky EJ, Xi L. Dietary nitrate supplementation protects against doxorubicin-induced cardiomyopathy by improving mitochondrial function. J Am Coll Cardiol 2011;57:2181–9.

81. Menna P, Salvatorelli E, Minotti G. Anthracycline degradation in cardiomyocytes: a journey to oxidative survival. Chem Res Toxicol 2010;23:6–10.

82. Zhang S, Liu X, Bawa-Khalfe T, et al. Identification of the molecular basis of doxorubicin-induced cardiotoxicity. Nat Med 2012;18:1639–42.

83. Lightfoot JC, D'Agostino RB, Hamilton CA, et al. Novel approach to early detection of doxorubicin cardiotoxicity by gadolinium-enhanced cardiovascular magnetic resonance imaging in an experimental model. Circ Cardiovasc Imaging 2010;3:550–8.

84. Jordan JH, D'Agostino RB, Hamilton CA, et al. Longitudinal assessment of concurrent changes in left ventricular ejection fraction and left ventricular myocardial tissue characteristics after administration of cardiotoxic chemotherapies using t1-weighted and t2-weighted cardiovascular magnetic resonance. Circ Cardiovasc Imaging 2014;7:872–9.

85. Weiss K, Schar M, Panjrath GS, et al. Fatigability, exercise intolerance, and abnormal skeletal muscle energetics in heart failure. Circ Heart Fail 2017;10:e004129.

86. Gupta A, Rohlfsen C, Leppo MK, et al. Creatine kinase-overexpression improves myocardial energetics, contractile dysfunction and survival in murine doxorubicin cardiotoxicity. PLoS ONE 2013;8:e74675.

87. Yusuf SW, Negi SI, Lenihan DJ. Infiltrative cardiomyopathy and pericardial disease. Semin Oncol 2013;40:199–209.

88. Sanon S, Lenihan DJ, Mouhayar E. Peripheral arterial ischemic events in cancer patients. Vasc Med 2011;16:119–30.

89. Desikan KR, Dhodapkar MV, Hough A, et al. Incidence and impact of light chain associated (AL) amyloidosis on the prognosis of patients with multiple myeloma treated with autologous transplantation. Leuk Lymphoma 1997;27:315–9.

90. Rajkumar SV, Gertz MA, Kyle RA. Primary systemic amyloidosis with delayed progression to multiple myeloma. Cancer 1998;82:1501–5.

91. Krombach GA, Hahn C, Tomars M, et al. Cardiac amyloidosis: MR imaging findings and T1

quantification, comparison with control subjects. J Magn Reson Imaging 2007;25:1283–7.

92. Feng D, Edwards WD, Oh JK, et al. Intracardiac thrombosis and embolism in patients with cardiac amyloidosis. Circulation 2007;116:2420–6.

93. Roberts WC, Waller BF. Cardiac amyloidosis causing cardiac dysfunction: analysis of 54 necropsy patients. Am J Cardiol 1983;52:137–46.

94. Neilan TG, Coelho OR, Shah RV, et al. Myocardial extracellular volume by cardiac magnetic resonance imaging in patients treated with anthracycline-based chemotherapy. Am J Cardiol 2013;111:717–22.

95. Tham EB, Haykowsky MJ, Chow K, et al. Diffuse myocardial fibrosis by T1-mapping in children with subclinical anthracycline cardiotoxicity: relationship to exercise capacity, cumulative dose and remodeling. J Cardiovasc Magn Reson 2013; 15:48.

96. Mewton N, Liu CY, Croisille P, Bluemke D, Lima JA. Assessment of myocardial fibrosis with cardiovascular magnetic resonance. J Am Coll Cardiol 2011;57:891–903.

97. Thompson RC, Canby RC, Lojeski EW, Ratner AV, Fallon JT, Pohost GM. Adriamycin cardiotoxicity and proton nuclear-magnetic-resonance relaxation properties. Am Heart J 1987;113:1444–9.

98. Cottin Y, Ribuot C, Maupoil V, et al. Early incidence of adriamycin treatment on cardiac parameters in the rat. Can J Physiol Pharmacol 1994; 72:140–5.

99. Meléndez GC, Jordan JH, D'Agostino RB Jr., Vasu S, Hamilton CA, Hundley WG. Progressive 3-month increase in left ventricular myocardial extracellular volume fraction after receipt of anthracycline based chemotherapy. J Am Coll Cardiol Img 2016;10:708–9.

100. Jordan JH, Vasu S, Morgan TM, et al. Anthracycline-associated T1 mapping characteristics are elevated independent of the presence of cardiovascular comorbidities in cancer survivors. Circ Cardiovasc Imaging 2016;9:e004325.

101. Toro-Salazar OH, Gillan E, O'Loughlin MT, et al. Occult cardiotoxicity in childhood cancer survivors exposed to anthracycline therapy. Circ Cardiovasc Imaging 2013;6:873–80.

102. Lunning MA, Kutty S, Rome ET, et al. Cardiac magnetic resonance imaging for the assessment of the myocardium after doxorubicin-based chemotherapy. Am J Clin Oncol 2013;21:1283–9.

103. Neilan TG, Coelho-Filho OR, Pena-Herrera D, et al. Left ventricular mass in patients with a cardiomyopathy after treatment with anthracyclines. Am J Cardiol 2012;110:1679–86.

104. Lawley C, Wainwright C, Segelov E, Lynch J, Beith J, Mccrohon J. Pilot study evaluating the role of cardiac magnetic resonance imaging in monitoring adjuvant trastuzumab therapy for breast cancer. Asia Pac J Clin Oncol 2012;8: 95–100.

105. Wadhwa D, Fallah-Rad N, Grenier D, et al. Trastuzumab mediated cardiotoxicity in the setting of adjuvant chemotherapy for breast cancer: a retrospective study. Breast Cancer Research and Treatment 2009;117:357–64.

106. Eckman DM, Stacey RB, Rowe R, et al. Weekly doxorubicin increases coronary arteriolar wall and adventitial thickness. PLoS ONE 2013;8: e57554.

107. Chow AY, Chin C, Dahl G, Rosenthal DN. Anthracyclines cause endothelial injury in pediatric cancer patients: a pilot study. J Clin Oncol 2006; 24:925–8.

108. Wolf MB, Baynes JW. The anti-cancer drug, doxorubicin, causes oxidant stress-induced endothelial dysfunction. Biochim Biophys Acta 2006; 1760:267–71.

109. Biglands JD, Magee DR, Sourbron SP, Plein S, Greenwood JP, Radjenovic A. Comparison of the diagnostic performance of four quantitative myocardial perfusion estimation methods used in cardiac MR imaging: CE-MARC substudy. Radiology 2015;275:393–402.

110. Greenwood JP, Maredia N, Younger JF, et al. Cardiovascular magnetic resonance and single-photon emission computed tomography for diagnosis of coronary heart disease (CE-MARC): a prospective trial. Lancet 2012;379:453–60.

111. Uren NG, Camici PG, Melin JA, et al. Effect of aging on myocardial perfusion reserve. J Nucl Med 1995;36:2032–6.

112. Wang L, Jerosch-Herold M, Jacobs DR, Shahar E, Folsom AR. Coronary risk factors and myocardial perfusion in asymptomatic adults: the Multi-Ethnic Study of Atherosclerosis (MESA). J Am Coll Cardiol 2006;47:565–72.

113. Ylänen K, Poutanen T, Savikurki-Heikkilä P, Rinta-Kiikka I, Eerola A, Vettenranta K. Cardiac magnetic resonance imaging in the evaluation of the late effects of anthracyclines among long-term survivors of childhood cancer. J Am Coll Cardiol 2013;61:1539–47.

114. Oberholzer K, Kunz RP, Dittrich M, Thelen M. Anthracycline-induced cardiotoxicity: cardiac MRI after treatment for childhood cancer. Rofo 2004; 176:1245–50.

115. Barthur A, Brezden-Masley C, Connelly KA, et al. Longitudinal assessment of right ventricular structure and function by cardiovascular magnetic resonance in breast cancer patients treated with trastuzumab: a prospective observational study. J Cardiovasc Magn Reson 2017;19:44.

116. Jordan JH, Castellino SM, Meléndez GC, et al. Left ventricular mass change after anthracycline chemotherapy. Circ Heart Fail 2018;11:e004560.

117. Coelho-Filho OR, Shah RV, Mitchell R, et al. Quantification of cardiomyocyte hypertrophy by cardiac magnetic resonance: implications for early cardiac remodeling. Circulation 2013;128:1225–33.

118. White CS. MR evaluation of the pericardium and cardiac malignancies. Magn Reson Imaging Clin North Am 1996;4:237–51.

119. Imazio M, Demichelis B, Parrini I, et al. Relation of acute pericardial disease to malignancy. Am J Cardiol 2005;95:1393–4.

120. Maisch B, Ristic A, Pankuweit S. Evaluation and management of pericardial effusion in patients with neoplastic disease. Prog Cardiovasc Dis 2010;53:157–63.

121. Kojima S, Yamada N, Goto Y. Diagnosis of constrictive pericarditis by tagged cine magnetic resonance imaging. N Engl J Med 1999;341:373–4.

122. Wang ZJ, Reddy GP, Gotway MB, Yeh BM, Hetts SW, Higgins CB. CT and MR imaging of pericardial disease. Radiographics 2003;23 Spec No:S167–80.

123. Zurick AO, Bolen MA, Kwon DH, et al. Pericardial delayed hyperenhancement with CMR imaging in patients with constrictive pericarditis undergoing surgical pericardiectomy: a case series with histopathological correlation. J Am Coll Cardiol Img 2011;4:1180–91.

124. Bogaert J, Francone M. Cardiovascular magnetic resonance in pericardial diseases. J Cardiovasc Magn Reson 2009;11:14.

125. Handke M, Schochlin A, Schafer DM, Beyersdorf F, Geibel A. Myxoma of the mitral valve: diagnosis by 2-dimensional and 3-dimensional echocardiography. J Am Soc Echocardiogr 1999;12:773–6.

126. Nishimura RA, Otto CM, Bonow RO, et al. 2014 AHA/ACC guideline for the management of patients with valvular heart disease: a report of the American College of Cardiology/American Heart Association Task Force on Practice Guidelines. J Am Coll Cardiol 2014;63:e57–185.

127. Caspar T, El Ghannudi S, Ohana M, et al. Magnetic resonance evaluation of cardiac thrombi and masses by T1 and T2 mapping: an observational study. Int J Cardiovasc Imaging 2017;33: 551–9.

128. Pazos-Lopez P, Pozo E, Siqueira ME, et al. Value of CMR for the differential diagnosis of cardiac masses. J Am Coll Cardiol Img 2014;7: 896–905.

129. Fussen S, De Boeck BW, Zellweger MJ, et al. Cardiovascular magnetic resonance imaging for diagnosis and clinical management of suspected cardiac masses and tumours. Eur Heart J 2011;32: 1551–60.

130. Staab W, Bergau L, Schuster A, et al. Detection of intracardiac masses in patients with coronary artery disease using cardiac magnetic resonance imaging: a comparison with transthoracic echocardiography. Int J Cardiovasc Imaging 2014;30:647–57.

131. Chan AT, Plodkowski AJ, Pun SC, et al. Prognostic utility of differential tissue characterization of cardiac neoplasm and thrombus via late gadolinium enhancement cardiovascular magnetic resonance among patients with advanced systemic cancer. J Cardiovasc Magn Reson 2017;19:76.

132. Zucchetti G, Rossi F, Chamorro Vina C, Bertorello N, Fagioli F. Exercise program for children and adolescents with leukemia and lymphoma during treatment: a comprehensive review. Pediatr Blood Cancer 2018;65:e26924.

133. Mijwel S, Backman M, Bolam KA, et al. Highly favorable physiological responses to concurrent resistance and high-intensity interval training during chemotherapy: the OptiTrain breast cancer trial. Breast Cancer Res Treat 2018;169:93–103.

134. Yu AF, Jones LW. Modulation of cardiovascular toxicity in Hodgkin lymphoma: potential role

and mechanisms of aerobic training. Future Cardiol 2015;11:441–52.

135. Yu AF, Jones LW. Breast cancer treatment-associated cardiovascular toxicity and effects of exercise countermeasures. Cardiooncology 2016;2:1.

136. Haykowsky MJ, Beaudry R, Brothers RM, Nelson MD, Sarma S, La Gerche A. Pathophysiology of exercise intolerance in breast cancer survivors with preserved left ventricular ejection fraction. Clin Sci (Lond) 2016;130:2239–44.

137. Levelt E, Rodgers CT, Clarke WT, et al. Cardiac energetics, oxygenation, and perfusion during increased workload in patients with type 2 diabetes mellitus. Eur Heart J 2016;37:3461–9.

138. AlGhatrif M, Zane A, Oberdier M, et al. Lower mitochondrial energy production of the thigh muscles in patients with low-normal ankle-brachial index. J Am Heart Assoc 2017;6: e006604.

139. Ahles TA, Root JC. Cognitive effects of cancer and cancer treatments. Annu Rev Clin Psychol 2018;14:425–51.

140. van Elderen SG, Brandts A, van Der Grond J, et al. Cerebral perfusion and aortic stiffness are independent predictors of white matter brain atrophy in type 1 diabetic patients assessed with magnetic resonance imaging. Diabetes Care 2011; 34:459–63.

141. Cottin Y, Touzery C, Coudert B, et al. Impairment of diastolic function during short-term anthracycline chemotherapy. Br Heart J 1995;73: 61–4.

142. Lapinska G, Kozlowicz-Gudzinska I, Sackiewicz-Slaby A. Equilibrium radionuclide ventriculography in the assessment of cardiotoxicity of chemotherapy and chemoradiotherapy in patients with breast cancer. Nucl Med Rev Cent East Eur 2012;15:26–30.

143. Feola M, Garrone O, Occelli M, et al. Cardiotoxicity after anthracycline chemotherapy in breast carcinoma: effects on left ventricular ejection fraction, troponin I and brain natriuretic peptide. Int J Cardiol 2011;148:194–8.

144. Stoodley PW, Richards DA, Hui R, et al. Two-dimensional myocardial strain imaging detects changes in left ventricular systolic function immediately after anthracycline chemotherapy. Eur J Echocardiogr 2011;12:945–52.

KEY WORDS cardio-oncology, cardiovascular magnetic resonance, tissue characterization

APPENDIX For supplemental videos, please see the online version of this paper.